Journal of Environmental Management 317 (2022) 115332

Contents lists available at ScienceDirect

Journal of Environmental Management

journal homepage: www.elsevier.com/locate/jenvman

Research article

Towards passive bioremediation of dye-bearing effluents using hydrous ferric oxide wastes: Mechanisms, products and microbiology

Pallavee Srivastava [a,*,1], Safaa A. Al-Obaidi [a,1], Gordon Webster [b], Andrew J. Weightman [b], Devin J. Sapsford [a]

[a] School of Engineering, Cardiff University, Queen's Building, The Parade, Cardiff, CF24 3AA, United Kingdom
[b] School of Biosciences, Cardiff University, Sir Martin Evans Building, Museum Avenue, Cardiff, CF10 3AX, United Kingdom

A B S T R A C T

A novel, circular economy-inspired approach for the "passive" (non-powered and reagent-free) treatment of dye-bearing effluent is presented. The treatment utilises the biogeochemical interaction of dye-bearing wastewater with hydrous ferric oxide (HFO) bearing sludges. The work presented demonstrates for the first time the reuse of HFO-rich waste sludges from potable water and mine water treatment. The waste was used directly without modification or reagent addition, as media/substrate in simple flow-through reactors for the decolourisation and biodegradation of methyl orange (MO) and mixed dyes textile effluent. Three phases of exploratory proof of concept work were undertaken. Columns containing HFO sludges were challenged with solution of MO, and MO amended with glycerol (Phase I), MO in a synthetic textile effluent recipe (Phase II), and real mixed textile effluent containing a mixture of dyes (Phase III). After an initial lag period extensive decolourisation of dye was observed in all cases at rates comparable with pure strains and engineered bioreactor processes, with evidence of biodegradation beyond simple cleavage of the mono azo chromophore and mineralisation. The microbiology of the initial sludge samples in both cases exhibited a diverse range of iron oxidising and reducing bacteria. However, post experiment the microbiology of sludge evolved from being dominated by *Proteobacteria* to being dominated by *Firmicutes*. Distinct changes in the microbial community structure were observed in post-treatment MWTS and WTWS where genera capable of iron and sulphate reduction and/or aromatic amine degradation were identified. Average nitrogen removal rates for the columns ranged from 27.8 to 194 g/m^3/day which is higher than engineered sequential anaerobic-aerobic bioreactor. Postulated mechanisms for the fast anaerobic decolourisation, biodegradation, and mineralisation of the dyes (as well nitrogen transformations) include various direct and indirect enzymatic and metabolic reactions, as well as reductive attack by continuously regenerated reductants such as Fe(II), HFO bound Fe(II), FeS, and HS^-. The ability of iron reducers to degrade aromatic rings is also considered important in the further biodegradation and complete mineralisation of organic carbon. The study reveals that abundant and ubiquitous HFO-rich waste sludges, can be used without amendment, as a substrate in simple flow-through bioremediation system for the decolourisation and partial biodegradation of dyes in textile effluent.

1. Introduction

Dye-bearing wastewater arise from dye manufacture, the printing industry, and pharmaceuticals production. However, it is the globally important textile industry that consumes most dye. The cloth and yarn dyeing processes use 30–50 L/kg and 60 L/kg, respectively (Kant, 2012; Ananthashankar and AuthorAnonymous, 2013). The wastewater arising from dyeing and fabric finishing typically accounts for circa 15–25% of textile wastewater (Garg et al., 2020; Kant, 2012). The dye lost during the dyeing process is estimated around 10–25%, whilst the unused dye that is directly discharged accounts to 2–20% (Carmen and Daniel, 2012). Dye-bearing textile wastewaters contain auxiliaries and sizing agents, and so are often highly alkaline, highly saline (Khalid et al., 2012) with elevated nitrogen concentrations because of urea and ammonia utilization (Chan et al., 2009). More than 50% of the estimated 280,000 tons of dyes discharged annually are azo dyes (Kalyani et al., 2009). Textile industries are economically significant and important in countries including the EU, China, Bangladesh, Vietnam, Sri Lanka, Mauritius, India, Turkey, and Nigeria (Khalid et al., 2012; Ananthashankar and AuthorAnonymous, 2013). In some cases, factories lack any

Abbreviations: HFO, Hydrous ferric oxide; MO, Methyl orange; MWTS, Mine water treatment sludge; WTWS, Potable water treatment works sludge; TC, Total carbon; TOC, Total organic carbon; HRT, Hydraulic retention time; COD, Chemical oxygen demand; EC, Electrical conductivity; DO, Dissolved oxygen; ORP, Oxidation-reduction potential; ICP-OES, Inductively coupled plasma optical emission spectrometer; LC-MS, Liquidchromatography-mass spectrometry; GC-MS, Gaschromatography-mass spectrometry; NGS, Next-generation sequencing; OTUs, Opertaional taxonomic units; 4-ABS, 4-aminobenzene sulfonic acid; N-DPD, N,N-dimethyl-p-phenylenediamine; RT, Retention time; WWS, Wastewater treatment sludge; EBCT, Empty bed contact time; NHRT, Nominal hydraulic retention time.

* Corresponding author.
E-mail address: srivastavap5@cardiff.ac.uk (P. Srivastava).
[1] Both authors contributed equally.

https://doi.org/10.1016/j.jenvman.2022.115332
Received 7 January 2022; Received in revised form 14 April 2022; Accepted 14 May 2022
Available online 23 May 2022

kind of effluent treatment plant. Treatment of dye-bearing wastewaters that is low-cost, sustainable, and appropriate to the economic setting are desirable.

Conventional wastewater treatment technologies are successfully applied for the treatment of dye-bearing textile wastewater. These include combinations of physical, and chemical unit operations, such as coagulation, electrocoagulation, adsorption, and advanced oxidation processes. These processes are expensive in terms of capital and operational costs, utilising expensive reagents, each with their own carbon footprint and generate secondary waste products such as sludge requiring management (Van Der Zee and Villaverde, 2005). Furthermore, they often require complex procedures and specialist knowledge. Biological approaches are comparatively inexpensive (Van Der Zee and Villaverde, 2005) and include anaerobic hydrolysis acidification, anaerobic/aerobic (A/O) or anaerobic/anoxic/aerobic (A2O) processes (Chen et al., 2019). However, these still require sophisticated process biotechnological control. As such, despite the existence of these established technologies, triple bottom line considerations, sustainable development goals, the continuing release of pollution (Mia et al., 2019), as well as the specific economic context continue to drive research into novel treatment methods.

"Passive" treatment methods (cf. "passive mine water treatment") involve methods with no continuous input of treatment reagents or energy, typically relying on natural microbiology (e.g. (Khandare and Govindwar, 2015),). Examples include treatment wetlands, phytoremediation, and simple flow through media bioreactors and/or photoreactors. Generally biological treatment involves anaerobic cleavage of the dye, followed by complete mineralisation under aerobic conditions. The limited success of passive methods explored to date, that remove between 50 and 80% with retention times of 7–10 days (Dhaouefi et al., 2018; Yaseen and Scholz, 2018) may partly be due to the lack of anaerobic stage.

Biogeochemical cycling has been recognised in the degradation of recalcitrant contaminants in wetland systems (e.g. (Han et al., 2020)) and implicated in the biodegradation of organic contaminants including BTEX, nitroaromatics, and dyes (Oon et al., 2018; Teramoto and Chang, 2019; Venosa and Zhu, 2003; Vymazal, 2007, 2013; Yadav et al., 2012). Iron oxides have been shown to have an important role in biodegradation of azo dyes promoting sulphate reducing bacteria, iron-reducing bacteria, and/or other microbes (Albuquerque et al., 2005; Li et al., 2017; Yu et al., 2016; Zhang et al., 2012). In the present study, waste hydrous ferric oxide (HFO)-bearing sludges and their extant microbial communities (hereon in 'HFO sludge') were utilised as substrate in a simple flow through system for assessment of dye biodegradation. These HFO sludges are common wastes arising from potable water treatment (the iron arising from the water/groundwater source itself, and/or added as coagulant), mine water treatment, and agricultural drainage (Bailey et al., 2013; Baken et al., 2013; R.E.Redmann, 1978; van Beek et al., 2020). With these sludges typically being landfilled, there are opportunities to develop industrial symbiotic and circular economy options for their reuse.

The present investigation was divided into three phases of work, with the aim of each phase as follows: Phase I, to determine whether the HFO sludge could degrade a simple azo dye, with Methyl Orange (MO) as a model, with and without additional labile carbon (glycerol) and to determine the influence of microbiology by comparing degradation with autoclaved controls; Phase II, to determine MO decolourisation and biodegradation under more challenging conditions of simulated textile effluent and low residence time; and Phase III, to determine the ability of HFO sludges to degrade and bioremediate real textile wastewater.

2. Materials and methods

2.1. HFO sludge collection and characterisation

Mine water treatment sludge (MWTS) was collected at a passive mine water treatment system located at the site of the former Lindsay colliery in Capel Hendre, Carmarthenshire, South Wales, UK. Common to most of the passive treatment system treating circumneutral, ferruginous coal mine water, the treatment system comprises of aeration cascades, settling ponds, and constructed wetlands. MWTS was collected from the bottom of the aeration cascade. Potable water treatment works sludge (WTWS) was collected from Hirwaun water treatment works in South Wales. The sludge was collected by bucket dipping from the sludge holding tank which holds HFO sludges from the site operations. Sludge samples were homogenised through hand-mixing and left to settle for 48 h, after which excess water was decanted. Sub-samples were taken and frozen at −80 °C for microbiological community analyses. The remaining wet sludge was stored at 4 °C prior to use. Chemical characterisation of both the sludges was undertaken by digesting ~0.1 g of the dried MWTS/WTWS in 6 mL aqua regia in a PTFE-lined ceramic vessel using a Multiwave 3000 (Anton Parr) microwave and analysed by ICP-OES (PerkinElmer Optima 2100). Total Carbon (TC) and total organic carbon (TOC) was measured using Total Organic Carbon analyser (TOC-V CSH (Shimadzu)). Dry weight, bulk density, dry density, specific gravity, and void ratio were determined according to BS 1377–2:1990. Mineral characterisation and sequential extraction data were supplemented from Roberts (2018).

2.2. Methyl orange measurement and sludge sorption capacity

All chemicals, standards, and reagents used in this work were purchased from Sigma Aldrich and Fisher Scientific. Methyl Orange (MO) was used as the model azo dye in Phase I and II of the experiments. Batch adsorption experiments were undertaken to determine the sorption capacity of MWTS HFO with respect to MO. Abiotic controls in which the MWTS was autoclaved at 121 °C, 15 PSI for 30 min (Prestige Medical 2100) and then gently dried at 40 °C for 48 h, were also run to exclude biological influence. Experiments were conducted using ~1.0 g of adsorbent in 100 mL MO solution under shaking conditions (150 rpm) at 15 °C and samples periodically withdrawn for analyses. A linear sorption response was found (Figure S1). The impact of background chemistry on adsorption capacity was determined using a single data point at 15 mg/L.

2.3. Column experiments

2.3.1. Phase I

Eight cylindrical acrylic columns (2.6 cm × 20 cm) were fabricated and stoppered at each end with bored rubber bungs with a quick fit adapter to connect plastic tubing. The columns were loaded with 128 g of wet MWTS, and glass wool was used to support and pack the remaining column void. Four of the columns were packed with **l**ive (L) unadulterated sludge, while the other four contained autoclave**d** (D) sludge (121 °C, at 15 PSI for 30 min: abiotic controls). Two types of influents were used: 15 mg/L MO prepared in deionised water (MO), and 15 mg/L MO amended with 0.46 g/L **g**lycerol (MO + GA) (Roberts, 2018). The columns were set up in duplicates as biotic with either MO (L) or MO + GA (L + G) as influents or abiotic with MO (D) or MO + GA (D + G) as influents. An eight-cassette peristaltic pump (used in this and all subsequent phases) was used to feed each column at a flow rate of 100 mL/day for 170 days, resulting in an Empty Bed Contact Time

Table 1
Review of various studies on methyl orange (MO) dye degradation in comparison to the present study.

Technique	Decolourisation %	Parameters	Notes	Reference
Anaerobic columns with HFO sludges; Phase I -MWTS autoclaved (D) or alive (L), with or without glycerol;	L + G- 95%; L- 92%; D + G- 90%; D- 50%	MO 15 mg/L HRT 22.8 h, T 15 °C, pH 5.5–8.0	HFO sludges present a good media for decolourisation of dye; sophisticated analysis of degradation product; effect of addition of additional carbon source determined; the role of indigenous microbial communities in dye decolourisation determined	Present study
Anaerobic columns with HFO sludges; Phase II – MWTS	98.9%;	MO 15 mg/L containing synthetic textile wastewater; HRT 1.66 h, T 15 °C, pH 7.0;		
Anaerobic columns with HFO sludges; Phase III- MWTS (M), WTWS (W), MWTS + WWS (MX)	M- 72%, W- 67%, MX- 82%	Real textile wastewater used as influent; HRT ~ 5 h, T 15 °C; pH ~ 10.0		
Anaerobic sequencing batch reactors	Partial decolourisation	MO 20 mg/L, sludge adsorption capacity 36 mg/g, adsorption contact time 10 min, pre acclimatising for 89 days, HRT 8–12 h, T 30 °C	Additional carbon source added; aromatic amines generated; HPLC and GC analysis	Yu et al. (2011)
Anaerobic sludge substrate from wastewater	90–96%	MO 50–150 mg/L, ORP -158 to −200 mV, pre- acclimatising 28 days, RT 24 h, at room temperature	Additional carbon source added; aromatic amines generated; spectrophotometer analysis	Murali et al. (2013a)
Integrated anaerobic- aerobic biofilm by activated wastewater sludge	95%	MO 50–300 mg/L, coconut fibre adsorption capacity 1.20 mg/g, ORP -100 to −169 mV, pre-acclimatisation 72 days, HRT 24 h	Additional carbon source added; aromatic amines generated; GC-MS spectrophotometer analysis	Murali et al. (2013b)
Anaerobic *Shewanella oneidensis*	80%	MO 100 mg/L, RT 16 h, T 30 °C, adsorption data neglected	Additional carbon source added; aromatic amines generated; HPLC-MS analysis	Cai et al. (2012)
Anaerobic *Kocuria rosea MTCC 1532*	100%	MO 10–70 mg/L, T 10–50 °C, RT 60 h	Additional carbon source added; aromatic amines generated; FTIR and GC-MS analysis	Parshetti et al. (2010)
Anaerobic *Aeromonas* sp. *strain DH-6*	100%	MO 100 mg/L, pH 3.0–7.0, T 5–45 °C	Additional carbon source added; aromatic amines generated; GC-MS and HPLC analysis	Du et al. (2015)
Anaerobic *Pseudomonas putida mt2* using a batch system	100%	MO 500 mg/L, T 35 °C, pH 7.0–9.0, dye removal 7.50 mg/g, RT 60 h	Additional carbon source added; aromatic amines generation not reported; spectrophotometry performed	Thao et al. (2013)
Anaerobic *Klebsiella oxytoca* using a batch system	100%	MO 32 mg/L, hematite, goethite Fe (III) was added as an electron acceptor, RT 24 h, T 25 °C	Additional carbon source added; aromatic amines not generated; spectrophotometry performed	Yu et al. (2015)
Aerobic mixed- bacteria *(E. coli* and *Enterobacter)* batch system	92%	MO 20 mg/L, pH 8.0, T 37 °C, RT 1 h	Additional carbon source added; aromatic amines not generation not reported; spectrophotometry performed	Rumky (2013)
Anaerobic baffled membrane bioreactor anaerobic wastewater sludge	100%	MO 50 mg/L, RT 23 h, pH 6.0–7.0	Additional carbon source added; aromatic amines not generated; LC-MS analysis	Liu et al. (2018)
Aerobic removal by bacterial consortium *Sphingomonas paucimobilis, Bacillus cereus*	92%	MO 750 mg/L, RT 48 h, pH 7, T 30 °C	Additional carbon source added; aromatic amines not generated; FT-IR and NMR analysis	Ayed et al. (2010)
Anaerobic sludge	100%	MO 70–300 mg/L, RT 12 h, T 30 °C	Additional carbon source added; aromatic amines generated; HPLC and GC were used	Yemashova et al. (2009)

Table 2
Operating parameters of bioremediation columns.

Phase of study	Column type	Sludge (g)	Flow rate (ml/day)	Number of days	EBCT (h)	NHRT (h)
Phase I	MWTS L + G	128	100	170	24.19	22.8
	MWTS L					
	MWTS D + G					
	MWTS D					
Phase II	MWTS	28	300	100	1.76	1.66
Phase III	MWTS	28	100	120	5.29	4.97
	WTWS				5.74	5.11
	MWTS + WWS				6.52	5.38

MWTS- Mine water treatment sludge; L + G-live column fed with glycerol amended influent; L-live column; D + G-autoclaved columns fed with glycerol amended influent; D-autoclaved column; WTWS- water treatment works sludge; WWS- wastewater treatment sludge.

(EBCT) of 24.19 h and a nominal Hydraulic Retention Time (HRT) of 22.92 h (Table 2). Laboratory temperature was monitored continuously (HANNA; HI141AH). Fig. 1 depicts the experimental setup for Phase 1. Effluent samples were collected daily. Concentrations of MO and Fe(II) were determined in column effluents daily (section 2.4), along with pH, electrical conductivity, redox potential, TC/TOC, and other elements as described in subsequent sections.

2.3.2. Phase II

Phase II also used MWTS as column media. Columns were fed with synthetic textile wastewater prepared according to O'Neill et al. (O'Neill et al., 2000). Briefly: One litre of deionised water contained 2.8 g modified starch, 530 mg acetic acid, 15 mg modified MO, 0.15 g NaCl, 0.23 g NH_4Cl, 0.28 g $(NH_4)_2SO_4$, 0.123 g $Na_3PO_4.12H_2O$, 0.038 g Na_2HPO_4, 2 g $NaHCO_3$. Both starch and dye were modified according to O'Neill et al. (O'Neill et al., 2000). This solution was amended with 1 mL of trace elements solution prepared as follows: 5 g $FeSO_4.7H_2O$, 0.0011g $ZnSO_4.7H_2O$, 0.1 g $MnCl_2.4H_2O$, 0.392 g $CuSO_4.5H_2O$, 0.248 g Co $(NO_3)_2.6H_2O$, 0.0177 g $NaB_4O_7.10H_2O$, and 0.025 g $NiCl_2$, per litre of water. Acrylic cylinders (2.5 × 10 cm) with screw top/bottom and inlet/outlet nozzles were packed with 28 g of MWTS using glass wool to

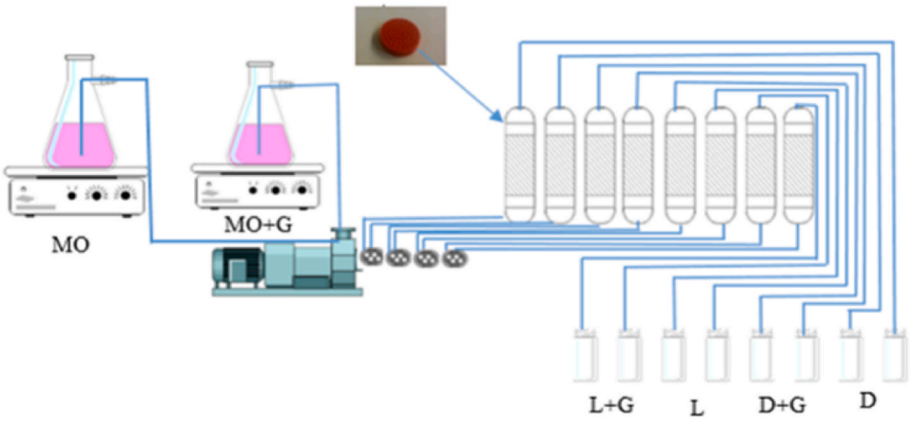

Fig. 1. Schematic of the phase 1 of the experimental set up. Methyl Orange (MO) and MO amended with glycerol (MO + G) were used as influents. Acrylic columns were packed with either fresh live MWTS (L) or autoclaved MWTS (D). These columns were fed with the influent via a peristaltic pump, and the effluents were collected in collection chambers labelled as L + G (live sludge fed with MO + G), L (live sludge fed with MO), D + G (autoclaved sludge fed with MO + G), and D (autoclaved sludge fed with MO). (For interpretation of the references to colour in this figure legend, the reader is referred to the Web version of this article.)

support and fill the void space. Columns were fed at a rate of 300 mL/day, resulting in an EBCT of 1.76 h and a nominal HRT of 1.67 h, notably lower than most textile wastewater studies. Duplicate columns were operated for 100 days at 25 °C, and samples withdrawn every 10 days to analyse various physical and chemical properties as per Phase I. SO_4^{2-}, NO_2^-, NO_3^-, NH_4^+, and Total Nitrogen (TN) were also determined, as described below (section 2.4).

2.3.3. Phase III

In Phase III of the experiments, MWTS and WTWS were used as column substrates. The influent used was real textile wastewater supplied by a cotton dyeing company and was stored at 4 °C until use. The wastewater was collected from the waste tank, which received dye wastewater from many processes, thus its exact composition is unknown. However, the various types of dyes and chemical compounds in use in the factory are given in Table S3. The effluent was characterised using the methods detailed herein and these are reported in Table S4. The columns were prepared as described above (2.3.2) and were packed with MWTS, WTWS, and MWTS mixed with autoclaved wastewater treatment sludge (WWS) in the ratio 9:1 (MWTS + WWS). A peristaltic pump was used to feed the columns with 100 mL/day for 120 days, giving an EBCT of 5.3 h for MWTS columns, 6.5 h for MWTS + WWS columns, and 5.7 h for WTWS columns. The nominal HRT for MWTS, MWTS + WWS, and WTWS obtained were 5.0 h, 5.4 h, and 5.1 h, respectively. The treated effluent was collected and characterised every 10 days, as in Phase I and II, supplemented with COD analysis.

2.3.4. Physico-chemical analysis of column effluents

pH, EC, dissolved oxygen (DO), and redox potential were measured using calibrated Mettler Toledo probes (InLab™ Expert Pro/LE703/605-ISM/InlabTM Redox ORP respectively). Inductively Coupled Plasma Optical Emission Spectrometer (ICP-OES; PerkinElmer Optima 2100DV) was used for selected elemental analyses on acidified samples (stored at 4 °C) after calibration with three commercial standards covering the detection range of the expected concentration for individual elements. A HACH DR900 colourimeter was used to determine concentrations (with dilutions as necessary) of ferrous iron (Fe(II)) (phenanthroline method), sulphate (SulfaVer reagent pillows), ammonium-nitrogen (Salicylate method), and COD (LC1400 COD cuvette test kit). Nitrite and nitrate analysis was carried out using the ICS-2000 ion chromatography system equipped with the AS18 detection column (maintained at 30 °C, total flow rate was 1 mL/min, an applied current of 57 mA, and an injection volume of 20 μL).

2.4. Degradation product analyses: spectrophotometry, LC-MS, and GC-MS

UV–Visible spectrophotometry (Hitachi, H-1900) was used to determine MO concentrations in deionised water (>18 MΩ) after filtration (0.45 μm filters). A linear 6-point calibration curve was obtained ($r^2 > 0.99$) using wavelength of 464 nm for MO (λ_{max} for the MO chromophore) (Jamshidi and Manteghi, 2020; Reeves et al., 1973). Calibration curves at pH 4.0 and pH 8.0 demonstrated a small difference and the response at pH 8.0 was used for MO concentration determinations. Dye degradation/adsorption was indicated by a decrease in absorbance of the effluent at 464 nm (λ_{max}).

Influent and effluents of the last week of the column experiments were analysed for degradation products using liquid chromatography-mass spectrometry (LC-MS). Waters LCT premier XE (ES/APCI ionisation) LC-MS was used for Phase I and II (operating condition reported in Table S5). ChemDraw software was used to analyse LC-MS data based on the m/z obtained to predict the chemical structure.

For Phase III, the samples were analysed using a LTQ Orbitrap XL 2 in both positive and negative mode (see Table S6). RemoteAnalyzer software was used to calculate the theoretical m/z values for all the possible compositions of carbon, hydrogen, oxygen, nitrogen, sulphur, and sodium in the chemical structure. A Clarus 500 GC-MS (PerkinElmer) equipped with a TurboMatrix head sampler HS 40/110 trap and Rtx-5 and amine fused silica columns (Crossband 5% diphenyl/95% dimethyl polysiloxane; RESTEK) was used to analyse effluent for the presence of dye degradation products (see section S1.1).

2.5. Microbial analysis

DNA was extracted from both the pre-test and the post-test HFO sludges using the "Fast DNA® SPIN Kit for Soil" (MP Biomedicals, Solon, OH, USA) as per the instruction manual, with slight modifications according to Webster at al. (Webster et al., 2003). The extracted DNA was quantified using the Qubit dsDNA assay kit (Invitrogen, Carlsbad, CA, USA) on the Qubit fluorimeter 3.0.

Next-generation sequencing (NGS) of bacterial and archaeal 16S rRNA genes was done on the Illumina MiSeq™ sequencer (Illumina, San Diego, CA, USA) following the EMP protocol (_1SIAP_ ; Caporaso et al., 2012). 16S V4 amplification primers with suitable Illumina adaptors were used (515F: 5′–AATGATACGGCGACCACCGAGATCTACACTATG GTAATTGTGTGCCAGCMGCCGCGGTAA, 806R: 5′–CAAGCAGAAGACG GCATACGAGATAGTCAGTCAGCCGGACTACHVGGGTWTCTAAT). The data generated by Illumina sequencing was analysed by QIIME v.1.8 (Caporaso et al., 2010). Sequence data was simultaneously

demultiplexed and quality filtered using default parameters of the program. The Operational Taxonomic Units (OTUs) were called using UCLUST with a 97% sequence similarity threshold. Taxonomy was then generated for the filtered sequences using BLAST and the SILVA 128 database (Altschul et al., 1990).

3. Results and discussion

3.1. Physicochemical and sorption characterisation of HFO sludges

The chemical and physical characteristics of the HFO sludges are given in Tables S1 and S2. The water content of MWTS, WTWS, and MWTS + WWS was 74%, 76%, and 80% respectively. MWTS exhibited a dry density of 2.87 g/cm^3 which is lower than that of ferrihydrite (3.96 g/cm^3), likely due to the presence of clay mineral fines (Schwertmann et al., 2003) and is comparable to other ochres in the South Wales coalfield (c.f. (Barnes, 2008)). The WTWS and MWTS + WWS exhibited a dry density of 1.17 and 1.03 g/cm^3, respectively. Fe was found to be the most abundant element (36.5% of DW) followed by Ca (1.8% of DW) in MWTS. WTWS on the other hand exhibited a lower Fe and Ca. Sequential extraction data indicated the majority of Fe to be in the easily reducible oxides and reducible oxides phases. XRD data indicated the presence of goethite, as well as a background peak at 35° 2θ corresponding to amorphous ferrihydrite. A small undulation at 62.5° 2θ was also observed which can be attributed to 2-line ferrihydrite (Singh et al., 2010). ~30% of the total iron was present within the 'magnetite targeted' phase, however magnetite was not identified as a phase by XRD.

The maximum MO removal due to adsorption from an initial 15 mg/L MO solution was 3.25 mg/g at pH 8.0. There was no significant difference between the contact times 3 h or 24 h in adsorption of dye. This value is comparable but slightly lower than those for textile wastewater treatment plant sludge of 36 mg/g (Yu et al., 2011) and agricultural wastes such as wheat bran and hog plum peel, of 12.33 mg/g and 20 mg/g, respectively (Alzaydien, 2015; Rumky, 2013). A maximum removal by sorption (in equilibrium with 15 mg/L MO) for each column was thus possible to be calculated from the sorption data and was 67.49 mg. Removal of MO in the columns that exceeds this value is attributable to biodegradation (see following sections).

3.2. Phase I

3.2.1. Decolourisation and effluent chemistry

The influent pH (4.5 ± 0.1) increased to ~pH 8.0 on passing through the MWTS column and this trend persisted throughout the experiment, except for L + G columns (Figure S2a). pH of L + G column changed to around pH 5.5 as the experiment progressed. The ambient temperature ranged between 10 °C and 24.5 °C, with an average of 15 ± 2.5 °C (Figure S2d). The redox potential for all the columns was approximately < -220 mV, indicating anaerobic conditions.

MO decolourisation was observed in all columns. Table 3 gives the rate of removals and the efficiency exhibited by all the columns. The columns exhibited dye removal efficiency in the following order: L + G > L ≥ D + G > D, where L + G columns exhibited the highest decolourisation efficiency (95%) and achieved the highest decolourisation rates (13.5 g/m^3/day). The efficiency of MO degradation exhibited by L + G columns is higher than those exhibited by other anaerobic sludge bioreactors or anaerobic fluidised bed (Murali et al., 2013a; Yu et al., 2011), and comparable to single organism anaerobic degradation studies (Parshetti et al., 2010; Thao et al., 2013; Yu et al., 2016). Table 1 exhibits comparison of various techniques and parameters used by this study to previous literature.

L + G columns became efficient in dye removal within 10 days of operation, whilst the L columns took around 2 months to achieve a similar decolourisation efficiency. L columns demonstrated a peak dye removal efficiency of 92% by day 60, which decreased to 50% by the end of the experiment (Fig. 2). The lowest dye removal efficiency was exhibited by columns packed with autoclaved MWTS without glycerol (D- 9.76%) at the end of the experimental period.

MO decolourisation was observed in all the columns from the inception of the experiments (Fig. 2), including the column packed with autoclaved media. This is consistent with removal by physicochemical sorption, as noted in the sorption experiment (Figure S1). Microbial decolourisation is thought unlikely in these early stages due to lack of acclimatisation time. In addition to sorption, the media may have contained a number of reductants such as Fe(II), Fe(II)-bound HFO, FeS (e.g. (Barnes, 2008; Roberts, 2018)), and green rusts (Bearcock et al., 2006; Roberts, 2018) which may have contributed to the initial decolourisation through reduction of the azo bond (Feng et al., 2000; Kone et al., 2009). As maximum removal of MO exceeded in all the cases (Table 1), adsorption cannot feasibly be the sole mechanism of MO removal. This implies biogeochemical removal mechanisms in addition to adsorption (cf. (Yu et al., 2011)) through which dye is decolourised enzymatically and indirectly through regeneration of reductants.

Autoclaved columns (D) exhibited the lowest dye removal rates when compared to non-autoclaved counterparts (Table 3) further corroborating the role of microbes in decolourisation. The autoclaved column supplemented with glycerol (D + G) demonstrated better dye removal/decolourisation than the non-supplemented column (D), indicating that additional carbon source stimulated decolourisation. The difference in decolourisation rates between the glycerol amended columns (L + G and D + G) indicated that autoclaving deactivated species important for MO decolourisation, and the final microbial communities in each column were different (see Section 3.2.3 below). It is notable that the pH of the L + G columns after ~30 weeks decreased to pH 5.5, lower than all other columns (See Figure S2a). This is probably due to production of acids from the fermentative biodegradation of glycerol (Clomburg and Gonzalez, 2013). That this pH change was not seen in the D + G columns (despite an extant community identified) demonstrates that autoclaving curtails acid production (remaining ~ pH 8.0 – see Figure S2a), but not decolourisation activity. This suggests that dye decolourisation is not dependent on specific acid-producing metabolic pathways and that MO decolourisation is comparable at pH 5.5 and 8.0. Previous studies exhibited pH between 6.0 and 10.0 to be optimal for dye decolourisation (Guo et al., 2007; Kiliç et al., 2007). Aromatic

Table 3
Various physico-chemical parameters of the column effluents.

Phase of study	Column type	Temp (°C)	DO (mg/l)	ORP (mV)	pH	Dye removal rate (g/m^3/day)	Efficiency	Total dye removed (mg)	Fe^{2+} conc. (mg/l)
Phase I	MWTS L + G	15	~8	−220	5.5	~13.0	95%	934.18	~10
	MWTS L	15	~8	−220	8.0	~13.0	92%	789.72	~0.2
	MWTS D + G	15	~8	−220	8.0	~12	73%	762.02	~0.15
	MWTS D	15	~8	−220	8.0	~9	54%	596.17	~0.24
Phase II	MWTS	15	<0.1	~-330	7.0	104	99%	164.49	~1.39
Phase III	MWTS	15	<1.0	ND	8.5	ND	72%	ND	0.5
	WTWS	15	<1.0		8.5		66%		0.9
	MWTS + WWS	15	<1.0		8.5		83%		0.8

ND- Not determined; MWTS- Mine water treatment sludge; L + G-live column fed with glycerol amended influent; L-live column; D + G-autoclaved columns fed with glycerol amended influent; D-autoclaved column; WTWS- water treatment works sludge; WWS- wastewater treatment sludge.

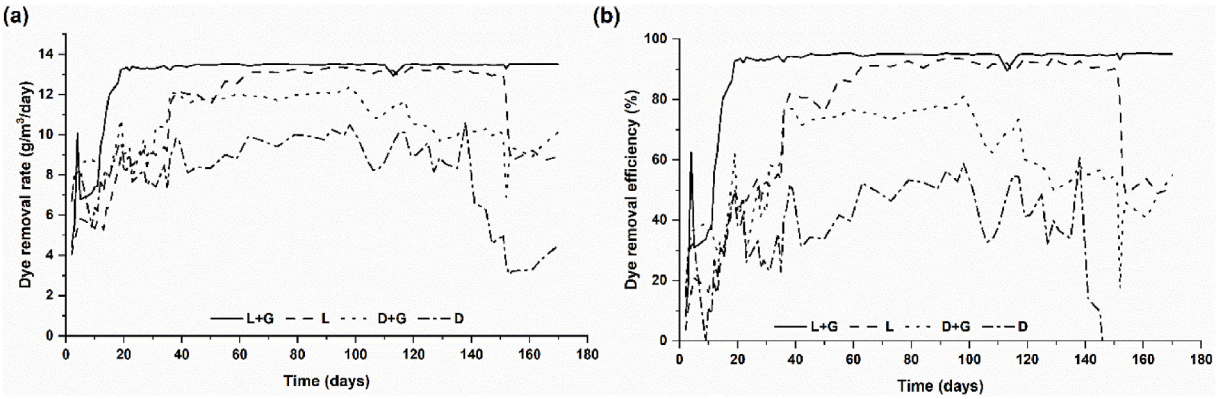

Fig. 2. The dye removal rate (a) and the dye removal efficiency (b) exhibited by the columns in phase 1 of the study, where L + G (live sludge fed with MO + G), L (live sludge fed with MO), D + G (autoclaved sludge fed with MO + G), and D (autoclaved sludge fed with MO).

amines, biodegradation products of azo dyes have been shown to increase the pH of the medium (Willmott, 1998).

Most interestingly, the L columns were able to decolourise the dyes to almost the same extent to the glycerol amended columns. Given that no other carbon source was added, this indicates that the microbial community can utilize MO and/or its breakdown products as electron donors in the system. In this system the continuous regeneration of azo reductants (e.g. Fe(II)) as products from iron reduction ensure continued MO decolourisation and resupply of MO breakdown products for continued iron reduction.

Temperature plays an important role in obtaining optimum biodegradation of the dye, as it influences the acclimatisation of the indigenous microbes and their enzyme activities (Saratale et al., 2011). Several studies have shown a higher temperature range between 35 and 40 °C for efficient biodegradation of dye (Guo et al., 2007; Wang et al., 2013). Although a lower temperature range between 15 and 30 °C was observed in this study (Figure S2d), higher rates of dye degradation were observed (See Tables 1 and 3).

3.2.2. C and Fe dynamics

TOC removal data for the columns showed that there was no significant removal for columns L or D, suggesting complete mineralisation of MO to inorganic carbon. The L + G and D + G glycerol supplemented columns exhibited TOC removal, commensurate with glycerol mineralisation within the columns. TOC in the L + G and D + G columns fluctuated between 204 and 165 mg/L and decreased to 140 mg/L. TC before and after in solid substrate did not increase (Table S1) indicating mineralisation to $CO_2/HCO_{(aq)}^-$ rather than accumulation in column media. Interestingly, the difference in effluent pH between L + G and D + G indicates different glycerol metabolism pathways and is reflected by differences in microbial community. The increase in TOC removal towards the latter part of the experiment coincides with decreased dye decolourisation/removal in the D + G columns suggesting that the glycerol degraders were the predominant species involved in dye decolourisation.

Iron released from MWTS into the effluent from L + G columns increased from 0 to 110 mg/L in the first two weeks, and thereafter fluctuated between 70 and 90 mg/L before reaching 120 mg/L total iron on day 170 (Figure S3a). Similarly, the release of Fe(II) was only observed in the effluent from L + G columns from day 1, peaking at 11 mg/L at the end of the experiment, see Figure S4. It is important to note that all the soluble iron released initially will be in the form of Fe(II), which oxidises rapidly at circum-neutral pH explaining the discrepancy. The export of Fe from the columns is indicative of microbial Fe(III) reduction which is corroborated by the identification of iron reducing bacteria such as *Geothrix* and *Geobacter* in these columns Similarly, Fe(II) release corelated with the observed dye decolourisation which could be due to Fe (II) acting as electron donor and improving enzyme activity in anaerobic columns, thereby enhancing dye degradation (Liu et al., 2012; Zhang et al., 2011). However, the other column effluents exhibited a total Fe concentration <1 mg/L. Ferrous iron was not detectable in D + G and D column effluents, while the L column effluents exhibited a Fe(II) concentration of 1 mg/L. The lower concentrations of Fe(II) in L column effluents may be due to sub-oxic conditions, oxidation of Fe(II), and precipitation of HFO, as indicated by the presence of Fe oxidising bacteria *Gallionella*.

ORP of the column effluents fluctuated between −170 mV and −250 mV (Figure S2c). The decrease in the oxidation-reduction potential is indicative of the reducing environment present in the columns amenable for iron reduction.

3.2.3. Microbiology

Useful dye degradation rates require acclimatisation of the indigenous consortia with dye and the harsh environment of the textile wastewater, along with optimal retention time, ideally more than the generation time of microbes (Comeau et al., 2016; Murali et al., 2013a). Several studies have shown that an acclimatisation of anywhere between 15 and 30 days increases the efficiency of the process to ~97% (Firmino et al., 2010; Thao et al., 2013; Zhang et al., 2012). In the present study, the acclimatisation time required by the indigenous MWTS consortia, in presence of an additional carbon source was 20 days, which in the presence of dye as the sole C source increased to 60 days.

Next Generation Sequencing (NGS) was used to carry out community analysis in the pre and post treatment columns (Fig. 3a). The predominant domain during the study in all the pre and post treatment columns was Bacteria (99.3%). However, during Phase I after 170 days of dye treatment the relative abundance of Archaea increased to 8% in L + G columns, whilst it was below the detection limit in L, and D + G columns. *Crenarchaeota* (0.59%) and *Euryarchaeota* (0.11%) were present in pre-test MWTS, of which *Crenarchaeota* could not be detected in any of the columns post treatment. *Euryarchaeota*, on the other hand exhibited an increase in relative abundance in L + G (7.93%) and L (0.93%) columns. *Proteobacteria* (63.84%) was the predominant bacterial phylum in pre-experiment MWTS followed by *Acidobacteria* (Fig. 3b). In the presence of glycerol, *Firmicutes* (72.15%) became the predominant phylum as compared to 0.47% in pre-test MWTS columns. Autoclaved column with glycerol (D + G) exhibited an increase in *Firmicutes* (45.5%) and *Proteobacteria* decreased to 34.6%. In MWTS columns without glycerol, *Proteobacteria* remained the predominant phyla followed by *Acidobacteria* (12.53%).

Although the four classes of *Proteobacteria* were present in the pre-test MWTS column (Figure S4a), *δ-Proteobacteria* accounted for 58.77% of the total *Proteobacteria*. While *α-Proteobacteria* could not be detected in L + G columns, the other classes of *Proteobacteria* also exhibited a decrease in relative abundance. MWTS column without

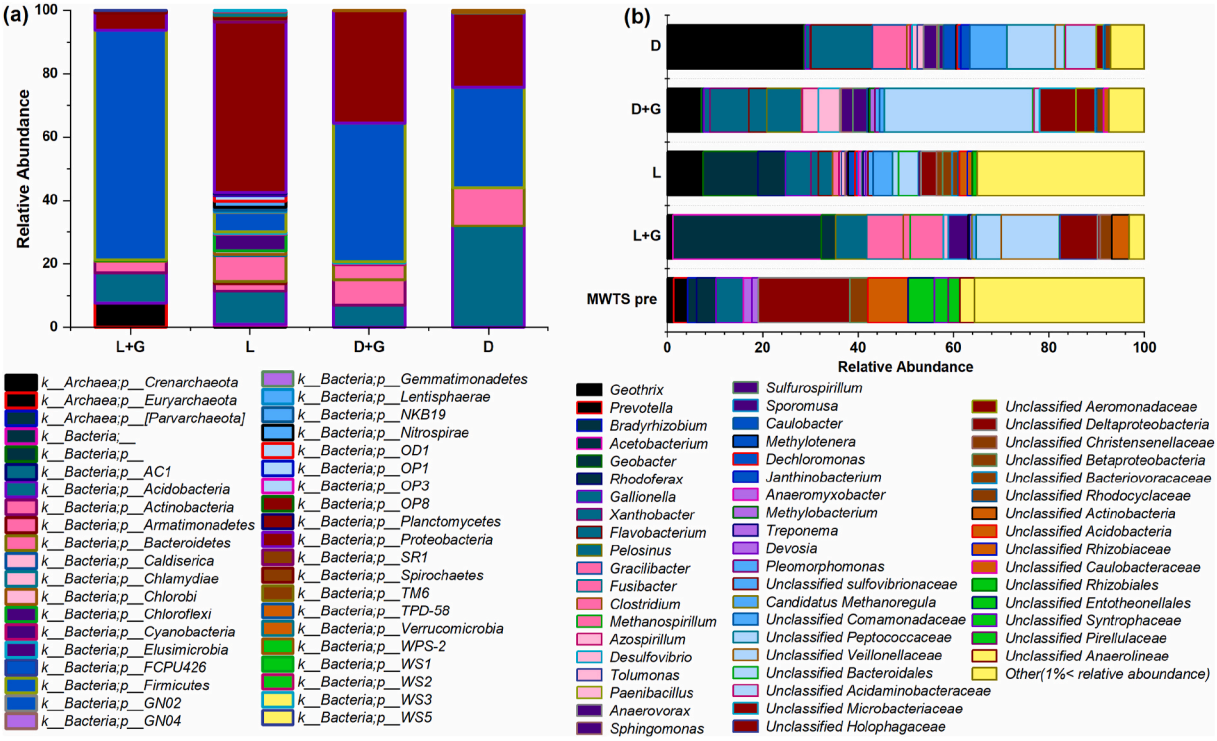

Fig. 3. Diversity of bacterial and archaeal 16S rRNA genes derived from columns in phase 1 of the study. (a) Relative abundance of microbes assigned at the phylum level in various column sludges post dye-degradation experiment. (b) Comparison of microbial diversity at the genus level in the sludge before and after dye-degradation. L + G (live sludge fed with MO + G), L (live sludge fed with MO), D + G (autoclaved sludge fed with MO + G), and D (autoclaved sludge fed with MO).

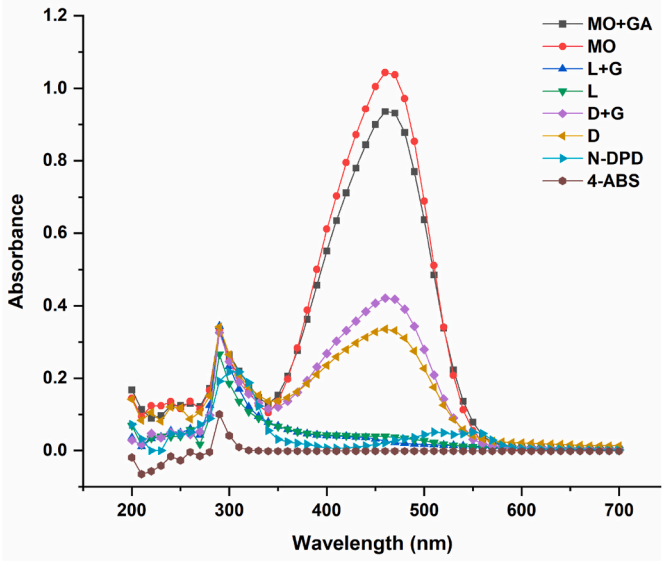

Fig. 4. Spectrophotometric analysis of the phase one effluents after 170 days of experimentation along with 15 mg/L Methyl Orange (MO), 15 mg/L MO amended with glycerol (MO + GA), N, N-dimethyl-p-phenylenediamine (N-DPD), and 4-aminobenzene sulfonic acid (4-ABS). L + G (live sludge fed with MO + G), L (live sludge fed with MO), D + G (autoclaved sludge fed with MO + G), and D (autoclaved sludge fed with MO). (For interpretation of the references to colour in this figure legend, the reader is referred to the Web version of this article.)

glycerol exhibited a relative increase in *β-Proteobacteria* and a slight decrease in *δ-Proteobacteria*. In both autoclaved columns with and without glycerol, the relative abundance of *Proteobacteria* was lower as compared to pre-test MWTS, however *γ- Proteobacteria* exhibited an increase. Two distinguished classes of *Acidobacteria* were identified, viz., *Holophagae* and *Acidobacteria*-6 (Figure S4b). *Acidobacteria*-6 accounted for 83.33% of the total *Acidobacteria* present in the pre-test MWTS column. However, this class could not be detected in L + G, D, and D + G columns, which only exhibited the presence of *Holophagae*. Amongst these three columns, D + G exhibited the highest relative abundance of *Holophagae*, followed by L + G, and D + G.

3.2.4. Degradation products and biodegradation pathways

The λ_{max} for methyl orange is 464 nm, while the influent exhibited two peaks at 290 nm and 464 nm. All the four types of columns used in phase I exhibited decolourisation of the wastewater (Fig. 4), as evident from the decrease in intensity of the peak at 464 nm. In fact, a complete disappearance of the dye chromophore peak was observed in the effluent of L + G columns. The MO peak at 290 nm remained unchanged from the influent in all the instances. The two commonly found MO degradation products reported in the literature, are 4-aminobenzene sulfonic acid (4-ABS) and N,N- dimethyl-p-phenylenediamine (N-DPD) (Yemashova and Kalyuzhnyi, 2006; Yu et al., 2011). To further establish dye degradation and not just decolourisation, the effluents were analysed spectrophotometrically between 200 nm and 700 nm and compared to 15 mg/L solutions of MO, 4-ABS, and N-DPD. Various studies have reported the presence of aromatic amines as an additional peak either at 226 nm or ~246 nm, post the cleavage of the azo bond (Cai et al., 2012; Murali et al., 2013a; Oturkar et al., 2011). However, no such additional peak was observed in any of the effluents, including the

effluents from D + G and D columns. Generation of aromatic amines is indicative of cleavage of the chromophore and may therefore be referred to as dye decolourisation, which is the usual fate of the dye during anaerobic textile wastewater treatment (Işik and Sponza, 2005; Kumar, 1998). Since no additional peaks of aromatic amines were obtained, this would suggest azo bond cleavage and opening of the aromatic ring (cf. (He et al., 2004)).

LC-MS and GC-MS were used to further characterise degradation products. MO in the influent wastewater eluted at 12.1–12.7 (or 10.9) min retention time (RT). This peak was absent in L + G column effluent, instead there were additional peaks observed at RT 10.2 min and 1.2 min. In case of L column effluents, the peak corresponding to MO was completely absent, and degradation product peaks were observed at 1.2 min. The intensity of the MO peak decreased in both the D + G and D column effluents, and an additional degradation product peak at RT 1.2 min was observed (Figure S5). The mass to charge ratio obtained from the LC-MS data was used to decipher the chemical structures of the degradation products (Table S7). As with the UV–Vis analyses, the usual degradation products of azo dyes, aromatic amines, were not detected. To further confirm the absence of aromatic amines, GC-MS was carried out using an amine column (Figure S6; Table S8). The common degradation product of MO, N-DPD could not be distinguished by GC-MS, while 4-ABS could not be identified as the boiling point of the compound was out of the GC-MS column range (Cai et al., 2012). Some studies have reported the peak for N-DPD at RT 9.84 min (Cai et al., 2012; Du et al., 2015; Parshetti et al., 2010), whilst some have observed it at RT 13.39 min (Murali et al., 2013a). Interestingly, a significant peak at RT 8.5 min was observed in L + G column effluent which can be attributed to 2 ethyl 1-hexanol ($C_8H_{18}O$) (Stein et al., 2011), its degradation product ethyl hexanoic acid is a known product of aromatic ring cleavage during dye degradation (Zhu et al., 2018). This peak was not observed in the effluents from L, D, and D + G columns. Although N-DPD and 4-ABS are the most widely reported degradation intermediates, few studies have also exhibited generation of various different intermediary products (Fan et al., 2011; Hisaindee et al., 2013).

Acetogenic *Firmicutes* such as *Sporomusa* and *Acetobacterium* were detected in the columns post treatment. These bacteria have been shown to degrade aromatic organic compounds (Delforno et al., 2016; Rosenberg et al., 2013) and may also be involved in the degradation of aromatic amines. The type of intermediates and the fate of the azo dye largely depends on the type of microorganism involved in biodegradation (Bheemaraddi et al., 2014; Chang et al., 2004). For instance, during a study on biodegradation of MO by *Aeromonas* sp., the aromatic amines generated at 12 h were found to be degraded by 24 h (Du et al., 2015). In another study on dye degradation in wetland, although 79% efficiency was reported in dye degradation, the indigenous consortia was unable to cleave the aromatic ring (Kadam et al., 2018).

Using the m/z ratio obtained by LC-MS and the ChemDraw software, the structures of various degradation products were obtained. These are indicative of broken azo bond and cleaved aromatic ring. Surprisingly,

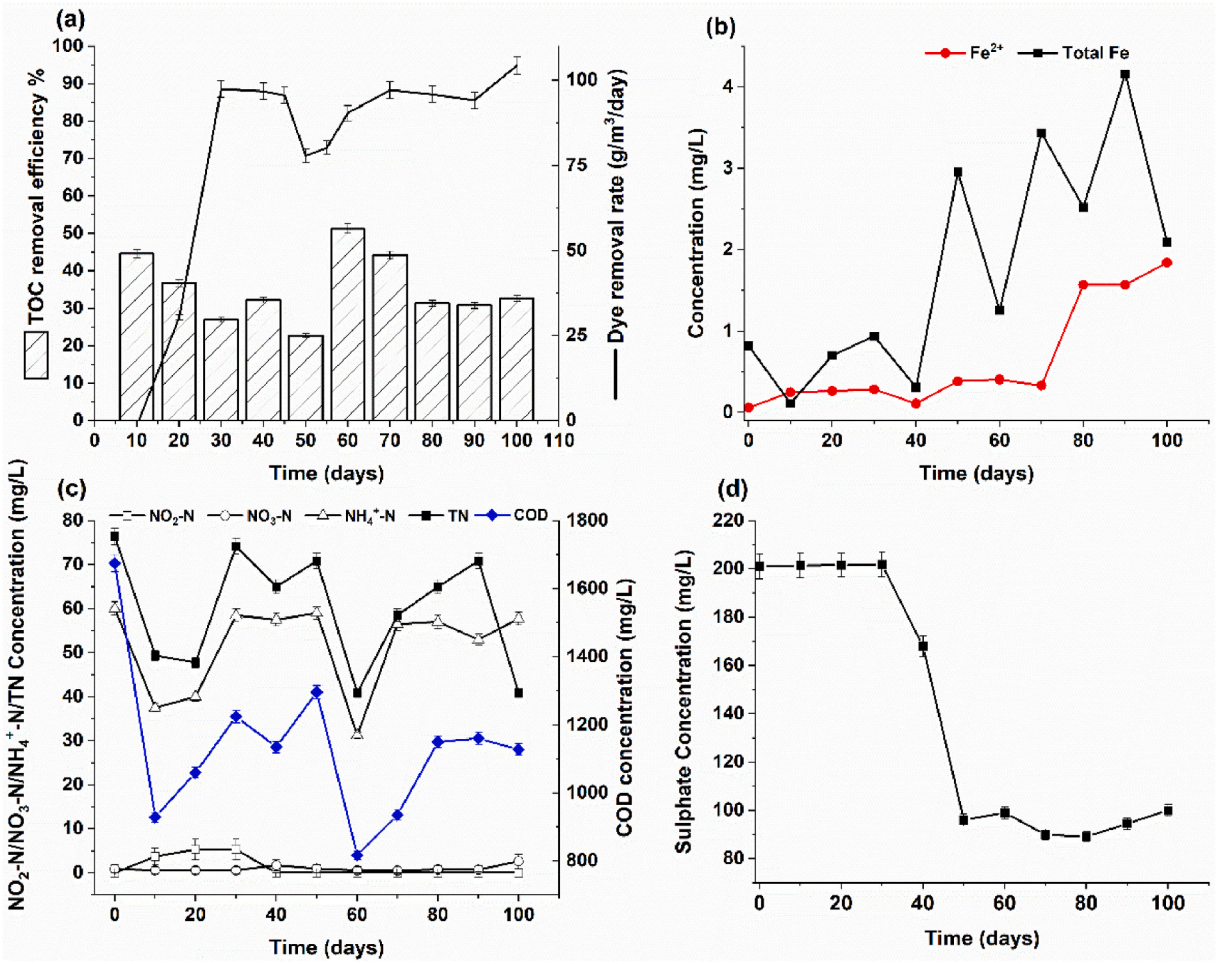

Fig. 5. (a) TOC removal efficiency exhibited by the MWTS columns with respect to the dye removal rate when synthetic textile wastewater was used as the influent; (b) Total iron and ferrous ion concentration in the effluents from MWTS packed columns; (c) Changes in the Total Nitrogen (TN), NO_2–N, NO_3–N, and NH_4^+-N concentrations with respect to COD concentration; (d) Sulphate concentration in the effluent from MWTS packed columns when synthetic textile wastewater was used as the influent.

distinct degradation products were also observed in effluents of autoclaved MWTS columns (D + G and D), likely as a result of few autoclave resistant microorganisms. *Firmicutes*, spore generating phyla, detected in both D + G and D columns, have been shown to biodegrade azo dyes (Schuppert and Schink, 1990).

Community analysis of the pre-test MWTS columns exhibited *Proteobacteria* as the predominant bacterial phyla that was taken over by *Firmicutes* post treatment with MO. Previous studies have shown that a consortium comprising of *Bacteroidetes*, *Proteobacteria,* and *Firmicutes* can result in anaerobic azo dye biodegradation (Rasool et al., 2016). In fact, *Proteobacteria* have been shown to degrade azo dyes as sole carbon source (Coughlin et al., 1999; Govindaswami et al., 1993), and the addition of carbon source enhanced the rate of azo dye degradation by *Firmicutes* (Yu et al., 2015). Iron reducing bacteria *Geothrix* and *Geobacter* were also identified in all the columns post treatment. *Geothrix* has been reported to be involved in iron reduction through both direct and indirect contact during MO degradation (Luu and Ramsay, 2003). *Geobacter,* an anaerobic iron reducing bacteria has been shown to mineralise organic aromatic contaminants (e^- donor) to CO_2, while reducing Fe(III) (e^- acceptor) (Lovley et al., 1993). *Clostridium* present in both L + G and L columms, has been shown to utilize the electron shuttle mechanism to reduce iron anaerobically (Fuller et al., 2014). *Pelosinus,* an anaerobic bacterium that uses glycerol as the organic C source and reduces metals (De León et al., 2015; Moe et al., 2012) was present in both L + G and D + G columns. A diverse variety of microorganisms acting in concert is key in degradation of aromatic amines (Arora, 2015; Nigam et al., 1996). Natural habitats such as sludge waste and soil are feasible substrates for azo dye degradation due to the diversity in the indigenous species present (Yu et al., 2011). Thus, the microbial diversity of MWTS exhibited efficient azo dye mineralisation, with L + G being most efficient.

3.3. Phase II

3.3.1. Decolourisation and effluent chemistry

The columns exhibited <50% dye removal in the first 10 days, as the experiment progressed the dye removal rate increased to 104.31 g/m^3/day exhibiting an efficiency of 98.97% (Fig. 5a). The effluent pH of the synthetic textile wastewater gradually declined from the influent value (pH 9.98) to pH 7.5 on day 20 and remained ~ pH 7.0 until the end of the experiment (Figure S7). Efficient textile wastewater treatment was observed between pH 6.5–10.0 (Chen et al., 2003). DO of the influent decreased from 3.47 mg/L on day 0 to almost 0 mg/L on day 20 and remained consistently <0.1 mg/L throughout the experiment. The temperature during Phase II averaged at ~15 °C.

The decrease in pH to values of ~7.0 is reflective of biodegradation and the formation of carbonic and organics acids. Starch present in the synthetic textile wastewater may be broken down to acetic, propionic, and butyric acids during azo dye degradation (Amaral et al., 2014). Redox potential varied between −250 mV and −350 mV (Figure S7), which is lower than that observed in Phase I but common to many studies on anaerobic biodegradation of azo dyes (Amaral et al., 2014; Bromley-Challenor et al., 2000; Georgiou et al., 2004).

The Phase II experiments took 30 days to reach 95–100% decolourisation, the lack of immediate effect may be related to the shock and longer acclimatisation time in the more challenging simulated textile wastewater and the much shorter residence time than Phase I. Thereafter, dye decolourisation increased to 100% for the duration of the experiment. This is promising as it shows when mixture of organics and nutrients are present, the dye biodegradation is fast and can be sustained even under high pH and saline conditions.

3.3.2. C/Fe/N/S dynamics

The influent synthetic textile wastewater exhibited a TOC of 1675 mg/L. The TC removal efficiency by the columns was between 22%–47% (Fig. 5a), with the highest removal rate of 9.198 g/kg/day observed on day 60. The pre-test TC of 1.53% accounted for the solid column substrate, which increased to 6.85% post-test (Fig. 8e), which could indicate filtration, also an important removal mechanism. Carbon removal rate has not been reported in majority of textile wastewater biodegradation studies. Several studies have reported that additional organic carbon source enhances the rate and efficiency of azo dye degradation (Anjaneyulu et al., 2005; García-Martínez et al., 2015; O'Neill et al., 2000). Starch present in the synthetic textile wastewater may act as the electron donor that may support anaerobic dye mineralisation (Carmen and Daniel, 2012).

Iron release in Phase II of the study was much lower as compared to that in phase I. There was a slow but steady increase in the concentration of total iron released in the effluent, which peaked at 4 mg/L on day 90. Similarly, the Fe(II) gradually increased from 0.3 mg/L on day 70 to 1.84 mg/L on day 100 (Fig. 5b). Low Fe(II) may be due to the low solubility of $Fe(OH)_2$, green rust, magnetite etc. at the observed elevated pH of the columns.

Total nitrogen along with N–NH_4^+, N–NO_3^-, and N–NO_2^- were monitored over the course of experiment. The synthetic textile wastewater used for Phase II contained 119.5 mg/L NH_4^+-N, 0.11 mg/L NO_3^--N, and 121.5 mg/L total N. Nitrite increased to 17.5 ± 0.7 mg/L by day 20, while the NH_4^+-N decreased to 40 ± 1.4 mg/L. NH_4^+-N removal efficiency ranged between 2.5% and 47.8%. The total nitrogen removal rate by the end of the experiment was 381 mg/kg/day exhibiting a removal efficiency of 46.5% (Fig. 5c). The nitrate concentration decreased in the first 20 days of the experiment indicating nitrification, with a simultaneous increase in nitrite concentration. Nitrification has been shown to occur during azo dye biodegradation when oxygen is available (Xiao et al., 2011). DO was seen to decrease only after day 20, which further supports the above. The presence of nitrite has been known to initiate ammonium oxidation (Annamox) (Isaka et al., 2007), which could be the reason behind the NH_4^+-N removal trend observed in this study. Furthermore, the abundance of iron oxides in the sludge along with the nitrogen compounds may provide an amenable environment for anaerobic ammonium oxidation coupled to Fe(III) reduction. This process where NH_4^+ oxidation occurs under iron reducing conditions, with iron oxide(s) serving as e^- acceptor is known as Feammox and has been shown to be an efficient method of nitrogen treatment (Le et al., 2021; Tian and Yu, 2020; W. H. Yang et al., 2012). The Fe(II) concentration post day 70 exhibited an increase with a simultaneous increase in ammonium nitrogen removal. Fe(II) reaction with NO_3^- and NO_2^- has also been reported to result in chemodenitrification (Buchwald et al., 2016) as too has FeS (Wei et al., 2017) and Fe(II) bound to HFO (Tai and Dempsey, 2009).

Sulphate decreased from 200 mg/L to 100 mg/L in the effluent after day 40 (Fig. 5d). This is a clear evidence of sulphate reduction. The likely fate of HS^- in the columns is reaction with HFO, forming iron monosulphides or reaction with the azo dye chromophore. Both HS^- and FeS can act as reductants for azo dyes (Li et al., 2021).

3.3.3. Microbiology

Introduction of the simulated textile wastewater to MWTS reduced the indigenous bacterial diversity by 75%, and archaeal diversity by 100%. The pre-dominant bacterial phyla in pre-test MWTS were *Proteobacteria* (61.24%), followed by *Acidobacteria* (9.98%), and *Chloroflexi* (7.44%). *Firmicutes* comprised of only 0.42% of the bacterial diversity in pre-test MWTS. Unlike Phase I, *Proteobacteria* did not drastically decrease in post-MWTS columns. Similarly, the relative abundance of *Firmicutes* increased to 34.24% in post-MWTS Phase II columns, which is lower than that exhibited by L + G columns in Phase I. The remaining bacterial phyla in the post-MWTS columns were *Bacteriodetes* (7.92%), *Actinobacteria* (3.93%), and others (0.04%). The microbial community structure at genus level in pre-test MWTS samples was distinct from that of post-test MWTS samples (Fig. 6).

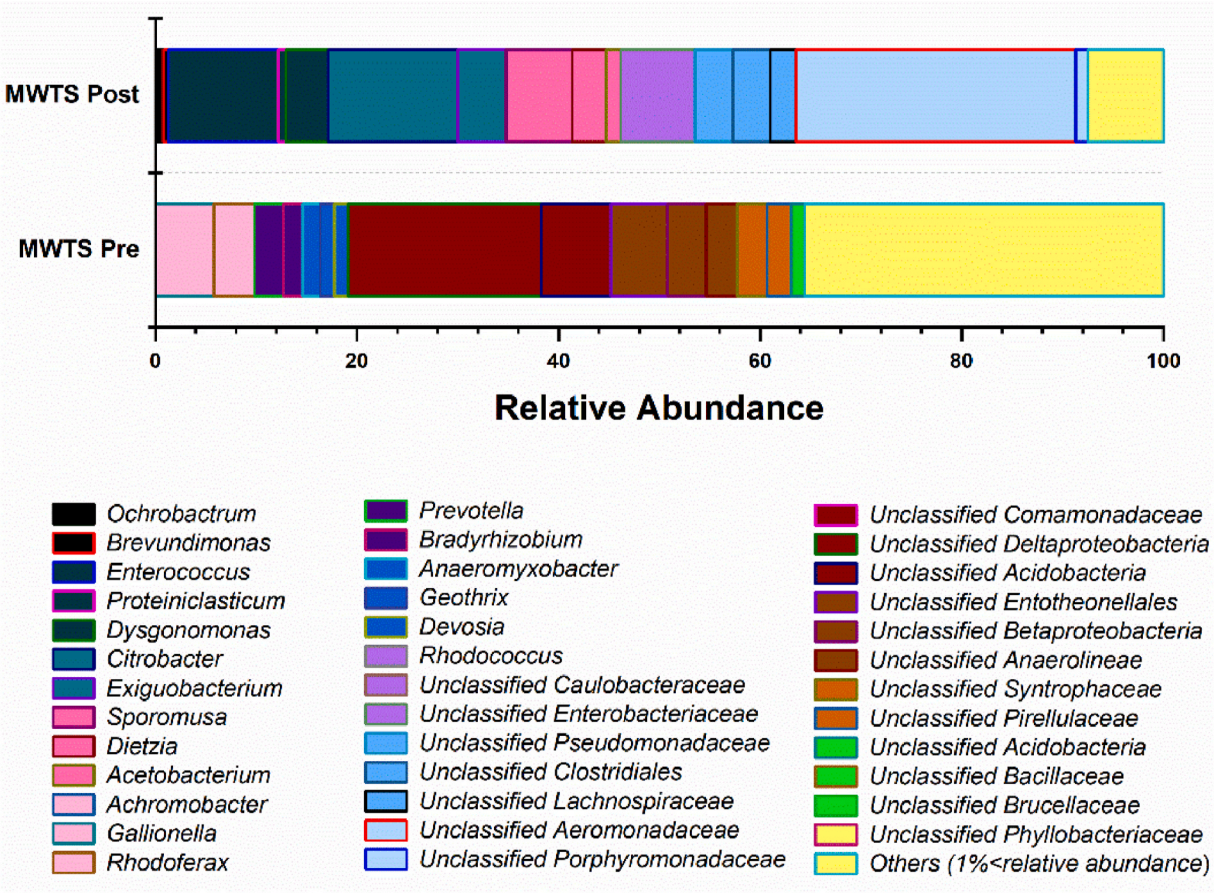

Fig. 6. Changes in microbial diversity at the genus level of MWTS before and after being exposed to synthetic textile wastewater.

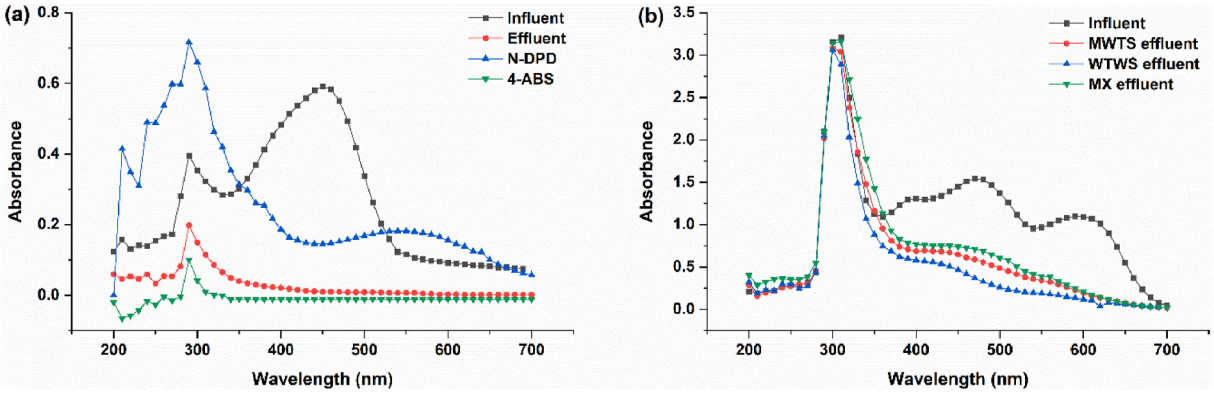

Fig. 7. Spectrophotometric analysis of (a) phase two effluents along with synthetic textile wastewater used as influent, N, N-dimethyl-p-phenylenediamine (N-DPD), and 4-aminobenzene sulfonic acid (4-ABS); (b) phase three effluents as compared to the real textile wastewater used as influent where MWTS is mine water treatment sludge, WTWS is water treatment works sludge, and MX is MWTS mixed with WWS (wastewater sludge) in a ratio of 9:1.

3.3.4. Degradation products and microbial pathways

The synthetic textile wastewater used in Phase II of the study exhibited peaks in absorbance at 300 nm and 464 nm (Fig. 7a). The peak at 464 nm, attributed to MO, was absent in the effluent indicating decolourisation of the dye. The aromatic amine peak at 249 nm was not detected. LC-MS analysis was carried out to further detect the degradation products (Figure S8). The influent exhibited peaks corresponding to MO at RT 16.8, 17.6, and 20 min. The intensities of these peaks decreased in the effluent, and three additional peaks were observed at 3, between 8 and 8.5, and between 13.8 and 14.6 min. Table S9 shows the degradation products of the synthetic textile wastewater as interpreted from the m/z and ChemDraw. Aromatic amines were not observed.

MWTS exhibited a 97.98% efficiency in synthetic textile wastewater decolourisation in four weeks. Limited decolourisation occurred in the first month of the experiment. High sulphate concentrations have been shown to inhibit azo dye colour removal (Ganesh et al., 1994). Decrease in sulphate concentrations presumably due to the onset of sulphate reduction are coincident with improvements in the efficiency of dye decolourisation. Other studies have only exhibited such efficiency when anaerobic degradation was followed by aerobic treatment (García-Martínez et al., 2015; Işik and Sponza, 2005). Efficient dye degradation is also dictated by the retention time, which was 1.66 h in this

experiment. Furthermore, neither the MO peak at 464 nm, nor the peaks corresponding to aromatic amines (250–300 nm) were detected in the MTWS effluent, suggesting the decolourisation of the azo dye and further breakdown of cleavage products.

As in Phase I, *Proteobacteria* was the predominant phyla in pre-test MWTS, however, post-treatment it remained the predominant phyla although there was a marginal decrease. This was closely followed by *Firmicutes*. Bacteria from these two phyla were effective in biodegradation of MO (Fig. 6). Plumb et al. (2001) found *Proteobacteria* and *Firmicutes* to be the primary phyla involved in azo dye degradation in an anaerobic reactor treating industrial dye effluent. Although *Citrobacter*, *Enterococcus*, *Sporomusa*, and *Dysgonomonas* were the predominant bacterial genera, *Ochrobactrum, Brevundimonas*, and *Proteiniclasticum* were also present in post-test MWTS. *Citrobacter* along with *Enterococcus* and *Ochrobactrum* have been shown to decolorise azo dyes (Khan et al., 2014). *Proteiniclasticum* has been known to degrade both the azo dyes and the aromatic amines (Zhu et al., 2018), which would explain the absence of these intermediate products in this study. Similarly, *Citrobacter* has also been shown to degrade the intermediary products generated during azo dye degradation (Chung et al., 1978). Given the high iron content of the sludge, the presence of *Sporomusa,* known for its ability to reduce Fe(III) present in HFO (Igarashi and Kato, 2021), is not surprising. *Enterococcus* in concert with iron reducing bacteria such as *Sporomusa,* have been shown to reduce Fe(III) to Fe(II) and cleave the azo bond (Bafana et al., 2009; Chen et al., 2004). Thus, the microorganisms present in post-test MWTS have previously shown capability for complete mineralisation of MO.

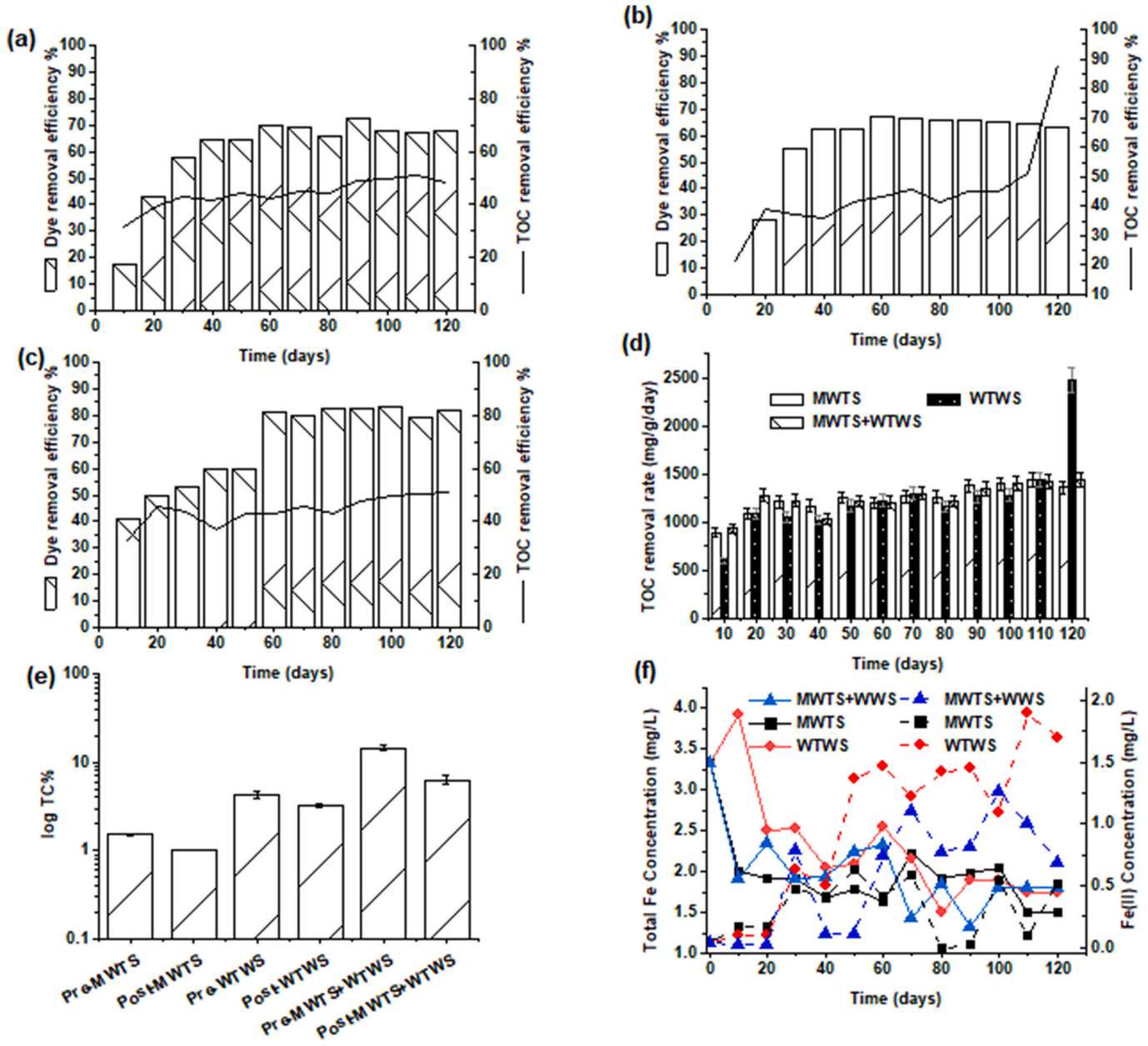

Fig. 8. Dye removal efficiency with respect to the TOC removal efficiency exhibited by (a) MWTS, (b) WTWS, and (c) MWTS + WWS packed columns; (d) TOC removal rate exhibited by columns in phase three of the study when real textile wastewater was used as the influent; (e) Changes in the total carbon (TC) content of various sludges pre- and post-the experiment; (f) Changes in the total iron and ferrous ion concentration over the course of experiment. (MWTS- mine water treatment sludge; WTWS- water treatment works sludge; WWS- wastewater treatment sludge).

3.4. Phase III

3.4.1. Decolourisation

This phase used real textile wastewater which comprised a mixture of various dyes and chemicals and exhibited an alkaline pH, high COD, TDS, and salinity (high Na, K, Cl^-, and SO_4^{2-}). HFO sludges MWTS and WTWS were used as column substrates in the following configuration: MWTS, WTWS, and MWTS + wastewater treatment sludge (WWS). Since the influent, i.e., the real textile wastewater was a mixture of dyes, it was imperative to determine the absorption maxima by spectrophotometry (see Fig. 7b). λ_{max} was determined to be 464 nm and was used as the wavelength to indicate dye decolourisation.

Prior to the actual decolourisation study, it was essential to test for dye adsorbed by MTWS, WTWS, and MWTS + WWS. Dye sorption may occur by diffusion, adsorption, or precipitation (Vadivelan & Vasanth Kumar, 2005). Once the active sites adsorbing the dye are saturated the dye sorption capacity declines (Doğan et al., 2004). In preliminary testing, the column substrates exhibited negligible dye decolourisation due to sorption. This is attributed to the highly alkaline and saline nature of the real textile wastewater (Namasivayam and Arasi, 1997). Any dye decolourisation observed would thus be a result of biodegradation.

The pH of the influent was 9.5 ± 0.2. Within first week of starting the reactors, the pH of MWTS columns dropped to 8.0, while WTWS and MWTS + WWS columns exhibited a pH of 8.1 and 9.1 respectively (Figure S9). Subsequently, the pH in all the columns remained at 8.5 ± 0.5. Studies on dye decolourisation using microorganisms have shown the process to occur either at highly alkaline or highly acidic conditions (Khan et al., 2014; Kiliç et al., 2007). The consistent pH observed may also suggest the absence of aromatic amines as biodegradation products because several studies have shown that generation of aromatic amines increases the pH of the effluent (Balapure et al., 2015; Wijetunga et al., 2010). The real textile wastewater exhibited a DO of 10 ± 1 mg/L which changed to <1 mg/L and remained so until the end of the experiment (Figure S9d). The temperature during the experiment ranged between 1 °C and 19.5 °C, with a slow increase to 15 °C (Figure S9).

In the first 10 days of the experiment, MWTS and WTWS columns exhibited negligible decolourisation, while MWTS + WWS column exhibited an efficiency of 40% in dye removal. MWTS + WWS columns were found to be most efficient in dye decolourisation followed by MWTS, and then WTWS (MWTS + WWS ≫ MWTS > WTWS; Fig. 8). The lag exhibited in dye decolourisation is indicative of the time required for the indigenous microbiota to acclimatise to the harsh environment. Since WWS is nutrient rich, the lag exhibited is lower than that of MWTS and WTWS. In fact, MWTS + WWS columns decolourised 82.9% of influent dye wastewater without any additional carbon source.

3.4.2. C/Fe/N/S dynamics

Although MWTS + WWS columns appear to be more efficient in TC removal in the first few days, all the three columns exhibited a 50% removal efficiency by the end of the experiment. The amount of TC present in the column substrates post-experiment was also lower, suggesting the mineralisation of C by the indigenous microorganisms (Fig. 8e). The real textile wastewater exhibited a TOC of 736 mg/L (Fig. 8a–d), which was actively mineralised as evident from the removal efficiency. The average mineralisation rate exhibited by these columns was 1250 g/m^3/day. Some studies have shown that microorganisms may degrade dyes as sole carbon source while some need an additional carbon source (Stolz, 2001; Telke et al., 2009). Real textile wastewater is usually rich in starch which acts as electron donor and has been shown to boost dye denaturation under anaerobic conditions (Van Der Zee and Villaverde, 2005). While other studies have shown that an additional carbon source exhibit a minor influence on the dye mineralisation process due to the competition of the additional carbon to be consumed rather than dye molecules (Saratale et al., 2011).

The total iron concentration in the real textile wastewater used as influent was 0.11 mg/L, which increased to 3.33 mg/L by day 10

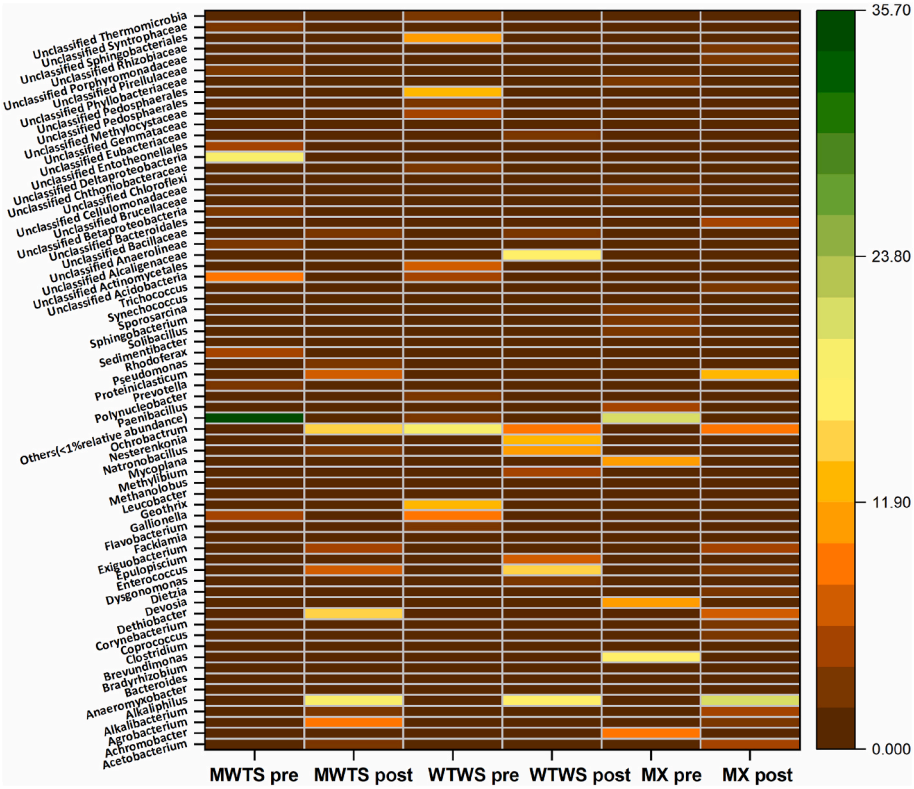

Fig. 9. Changes in microbial diversity observed in various sludges and their mixtures before and after dye-degradation studies. (MWTS- mine water treatment sludge; WTWS- water treatment works sludge; MX- MWTS mixed with WWS (wastewater sludge) in a ratio of 9:1).

(Fig. 8f). The Fe(II) concentration in the WTWS effluent by the end of the experiment was 1.34 mg/L, which was higher than that exhibited by MWTS (0.51 mg/L) or MWTS + WWS (0.69 mg/L). It is noteworthy that Fe(II) solubility is limited in the pH range of the column effluents (pH 8.5 ± 0.5).

NH_4^+-N, nitrate, and nitrite concentrations were determined in the influent and effluent to study the nitrogen transformations during dye biodegradation. Both MWTS and MWTS + WWS columns exhibited a dramatic decrease in NH_4^+-N in the first 10 days, after which the decrease was very gradual (Figure S10a-c). However, by the end of the experiment 95% of the NH_4^+ was removed. The simultaneous decrease in NH_4^+-N and increase in NO_2^- suggests nitrification, where ammonia is oxidised to nitrite. DO data supports the nitrification in the first 30 days, after which the system became anoxic for the next 50 days followed by anaerobiosis for the next 40 days. The nitrite generated by the ammonia oxidising bacteria was further oxidised by nitrite oxidising bacteria to nitrate (Annamox (Texier et al., 2012)). The final step is denitrification, where the nitrate is reduced to N_2, which requires anaerobic conditions (Texier et al., 2012). In Phase III, the sulphate concentration in the system largely remained unchanged through the course of the experiment, suggesting that sulphate reduction did not occur (Figure S10d).

3.4.3. Microbiology

Microbial community analysis of MWTS columns post treatment with real textile wastewater exhibited a decrease in microbial diversity by ~71% as compared to pre-treatment MWTS columns. As in Phase I, *Proteobacteria*, which was the predominant bacterial phylum in pre-test columns, decreased by 50% in post-test MWTS columns. As the experiment progressed, *Firmicutes* (67.09%) became the predominant bacterial phyla, followed by *Proteobacteria*. Fig. 9 shows the changes in bacterial diversity at genus level, pre- and post-treatment.

WTWS columns, before the treatment with real textile wastewater, exhibited a much higher microbial diversity which was significantly distinct from the MWTS columns. Treatment with real textile wastewater decreased the microbial diversity of WTWS columns by 53.85%. *Proteobacteria* (36.5%) were the predominant bacterial phyla pre-test and remained largely unaffected by the treatment with real textile wastewater. *Firmicutes* accounted for 50.91% of the entire bacterial diversity present in the post-WTWS columns. Fig. 9 shows the effect of the treatment of WTWS columns with real textile wastewater on the bacterial diversity at the genus level.

Treatment of MWTS + WWS columns with real textile wastewater resulted in a relative decrease in abundance with respect to pre-test by 40%. As in other columns, *Proteobacteria* (64.23%) was the predominant phylum, followed by *Firmicutes* (14.72%), *Bacteroidetes* (8.91%), *Chloroflexi* (6.12%), and *Actinobacteria* (4.48%). Post treatment with real textile wastewater, *Firmicutes* (62.09%) proliferated in the columns and *Proteobacteria* decreased to 17.71%. *Bacteroidetes* increased marginally to 10.55% and *Euryarchaeota* that was not detected in the pre-test columns were detected at 1.31%. The bacterial diversity of the post MWTS + WWS columns at genus level (Fig. 9) was distinctly different from that of any other columns studied here.

3.4.4. Degradation products and biodegradation pathways

Real textile wastewater with unknown dye composition exhibited a sharp peak at 300 nm and two broad peaks between 410 nm and 620 nm. The peak at 300 nm remained unchanged for all the column effluents, however the other two broad peaks in the visible range were absent. The MWTS + WWS column exhibited the best decolourisation efficiency (Fig. 7b). Aromatic amines as degradation products were not detected as evident from the absence of additional peaks between 200 and 400 nm, suggesting the breakdown of aromatic amines into aliphatic hydrocarbons (He et al., 2004). As the exact dye composition of the influent was unknown both positive and negative LC-MS were used to study dye degradation. Peaks observed in the influent in both positive (8–20 min RT and 13–31 min RT) and negative (0–11 min RT) LC-MS were not observed in the effluents of MWTS, WTWS, and MWTS + WWS columns (Figure S11 and S12). The general intensity of the peaks observed in the influent was found to decrease by 50% in the effluents of all three columns (as indicated by arrows in Figure S12). Peaks due to amine degradation products were not obtained, indicating not just dye decolourisation but complete biodegradation of the dyes by all three columns.

All the three columns exhibited the same trend in total iron content, whilst the Fe(II) was found to increase only marginally. Iron may have been reduced by organisms capable of iron reduction such as *Alkaliphilus*, and other *Firmicute* species. Fe(II) generated may react with NO_2^- obtained during ammonia oxidation forming Fe(III) that precipitates in the column thus exhibiting a marginal increase in Fe(II) concentrations (Ottley et al., 1997).

$$6Fe^{2+} + 2NO_2^- + 8H_2O \rightarrow 6FeOOH + N_2 + 10H^+ \quad (1)$$

Proteobacteria was the pre-dominant bacterial phyla in all the pre-test HFO sludges, which were taken over by *Firmicutes* post treatment. Studies have shown azo dye mineralisation under anaerobic conditions by a bacterial consortium comprising of *Firmicutes* (Wang et al., 2018). *Alkaliphilus,* a *Firmicute* was found to increase drastically in the post-test column substrates. It is a spore forming, anaerobic, iron-reducing bacteria, that has been shown to be efficient in azo dye mineralisation (Yang et al., 2011). Similarly, *Ochrobactrum,* which is usually enriched in iron contaminated soil have been known to degrade azo dye in concert with other bacteria (Khan et al., 2014).

In addition to iron-reducing bacteria, other genera such as *Dethiobacter* were observed. Representatives of this genus are known sulphate reducing bacteria found in iron rich soil (Sorokin et al., 2008). *Proteiniclasticum* and *Pseudomonas* were both detected in the column substrates and have been known to degrade both the azo bond and the intermediate aromatic amines to CO_2 and H_2O (Zhu et al., 2018). *Agrobacterium* present in MWTS and MWTS + WWS columns have been shown to degrade the aromatic amines produced during azo dye degradation (Silke et al., 1998). The presence of these genera supports the absence of aromatic amine peaks on the UV–Visible and the LC-MS scans. *Nesterenkonia,* detected in post-test WTWS are usually found in lake mud, and have been shown to cleave the azo bond at high pH and salinity (Bhattacharya et al., 2017). *Natronobacillus*, an anaerobic obligately alkalophilic, highly salt-tolerant natranophile was identified in both MWTS and WTWS columns post treatment. Similarly, *Exiguobacterium* and *Alkalibacterium* are halophilic and alkaliphilic bacterial genera present in the post-test columns, that have been shown to degrade azo dyes under hypersaline conditions (Forss et al., 2013). The real textile wastewater is highly alkaline and saline which would enrich these genera. *Achromobacter* and *Corynebacterium* found in post-test MWTS + WWS sludge are also known to degraded azo dye (Jin et al., 2015). *Enterococcus* a facultative anaerobic bacterium, present in all the three columns post-test, uses azoreductase to degrade the azo dye (Punj and John, 2009). *Trichococcus*, a facultative anaerobe, has been shown to be the dominant genus detected during azo dye degradation under iron-reducing condition (Wang et al., 2018). The enrichment of iron-reducing bacterial genera and the affiliated microorganisms with the capability to degrade both the azo bond and aromatic amines resulting in complete dye mineralisation is evident in the post-test HFO sludges.

3.5. Summary of feasible degradation mechanisms in HFO sludge reactors

The results of the experimental work demonstrate that HFO-bearing wastes and the associated microbial community within the simple flow reactors can decolourise MO. This was achieved with MO as a sole electron donor and in simulated textile effluent at rates higher (substantially lower residence time and high removal efficiency) than comparable studies in the literature that utilised more engineered systems and sometimes unique strains. Furthermore, the HFO system not only

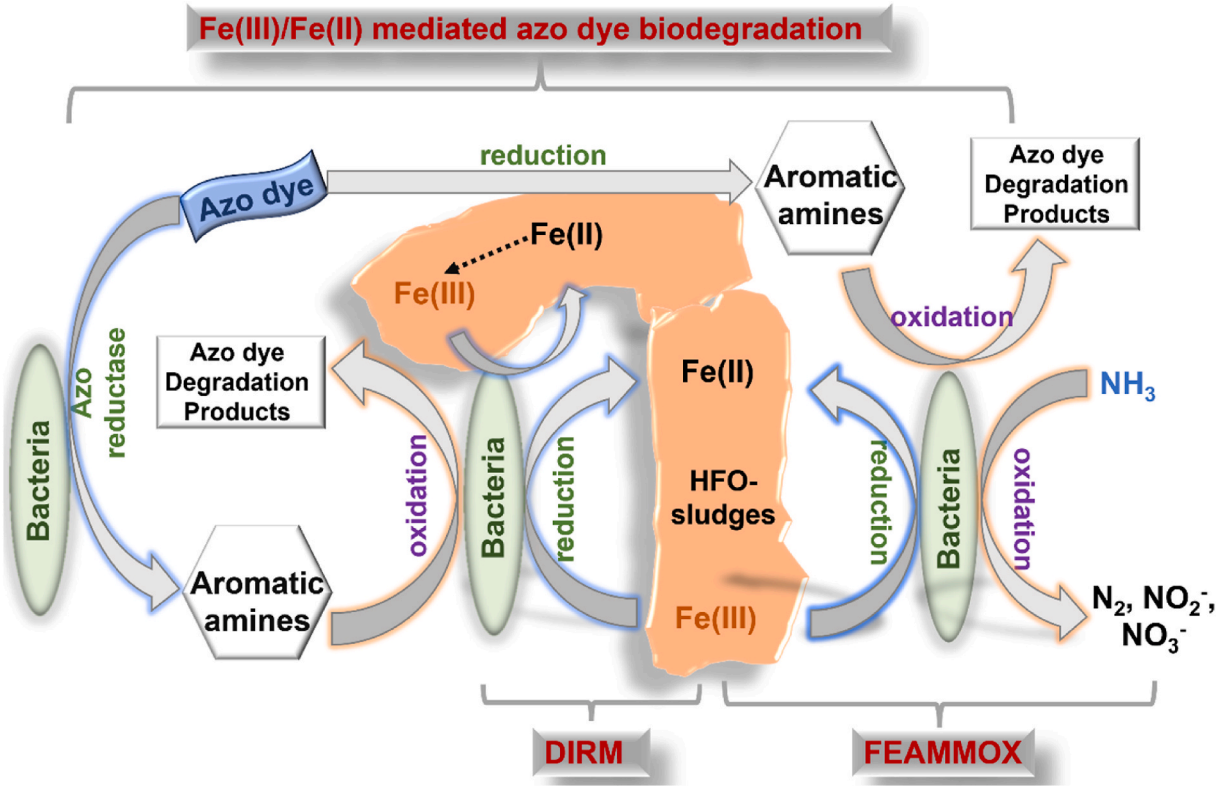

Fig. 10. Postulated mechanisms of complete dye degradation coupled with iron reduction: Iron reducing bacteria (*Geothrix*, *Geobacter*) present in HFO sludge reduce Fe(III) to Fe(II) that act as reductants for azo bond (eg. *Trichococcus*, *Enterococcus* in concert with *Sporomusa*). At the same time numerous bacteria were identified that are known to degrade azo bond using non-specific azo reductases and the resulting aromatic amines to CO_2 and H_2O (eg. *Proteiniclasticum*, *Alkalibacterium*). Nitrification associated with azo dye degradation induces ammonium oxidation which when coupled with dissimilatory iron reduction (DIRM) results in iron-mediated ammonia oxidation (FEAMMOX). This process also regenerates Fe(II) that further acts as reductant for azo bond cleavage.

Table 4
Summary of feasible biogeochemical routes to dye biodegradation in HFO-bearing column reactors.

Active agent/species	Production	Mechanism of dye decolourisation and/or biodegradation	Literature Example(s)
Assorted bacteria	Proliferation of bacteria under conditions within the columns	• Direct reductive enzymatic attack via low specificity cytoplasmic azo reductases and/or release of electron shuttles •Nonspecific bioreduction using azo dyes as electron acceptors •Some bacteria reported to use azo chromophore as an electron acceptor	See sections 3.2.4, 3.3.4 and 3.4.4 (Hong et al., 2007; Liu et al., 2016; Singh et al., 2015)
Fe-reducing bacteria		•Oxidation of recalcitrant organics including aromatics coupled to HFO bioreduction	
Fe(II)	Product of HFO bioreduction; reaction of HS^- with HFO	•Reductive attack cleaves chromophore	(Bafana et al., 2011; Guo et al., 2010)
FeOOH–Fe(II)	Surface mediated bioreduction of HFO involving interfacial electron transfer	•Species is a more powerful reductant than Fe(II) aq. Reductive attacks cleaves chromophore	(Elsner et al., 2004; Tobler et al., 2007)
FeS	Product of reaction of HS^- with HFO	•Reductive attack cleaves chromophore	
HS^-/H_2S	Product of bioreduction of sulphate associated with HFO or influent		(Kim et al., 2008; Yoo, 2002)
Bio- and bionanomagnetite	Known reaction product of HFO bioreduction		e.g. (Pattrick et al., 2013)
Green rust	Known reaction product of HFO bioreduction		Kone et al., (2009)
Electron shuttles and redox mediators	Humic acids/organics present in WWS/or released from bacteria	•Facilitation of bioreduction of HFO and chromophore	(Guo et al., 2010; Liu et al., 2011)
Reactive Oxygen Species (especially OH^-)	Produced by oxidation of Fe(II) and mineral-bound Fe (II) at redox boundary, hydroxy and superoxide radical $OH^·$ radical production upon reoxidation of Fe(II) degrades aromatic structures	•Oxidative attack on organic compounds, degradation of aromatic ring	Han et al., (2020)

led to cleavage of the chromophore, decolourising the dye but there was also clear evidence of further anaerobic biodegradation, as none of the cleaved MO products were detected in any of the systems. This is significant because usually the aromatic amines generated by MO degradation require degradation by aerobic treatment to less toxic compounds (Breithaupt et al., 2003; Brown and Hamburger, 1987; Ganesh et al., 1994; Pandey et al., 2007). According to Pinheiro et al. (2004) "only a few of the studies on microbial azo dye reduction included a clear demonstration of total or partial, subsequent biodegradation of the resulting metabolites, aromatic amines".

The excellent results observed for dye degradation in the presence of HFO- sludges require further explanation, and there are many plausible biogeochemical reactions which could contribute to the decolourisation and further biodegradation of products (Fig. 10). Sections above highlight the range of microbial species present which have known ability to either decolourise dyes (through non-specific azoreductase enzymes) or degrade recalcitrant organic species, breaking the aromatic ring. Many of these are iron-reducing organisms which would clearly be expected to thrive under anaerobic conditions and in the presence of an excess of reactive Fe(III) in the form of HFO. There are many other chemical species within the system which likely can decolourise, degrade, or mineralise azo dye and its breakdown products. These are summarised in Table 4.

4. Conclusions

This study demonstrates the decolourisation and biodegradation of methyl orange and mixed dyes from a real textile wastewater with HFO-bearing waste sludges arising from potable water and mine water treatment. Both the rates of decolourisation and the extent of anaerobic biodegradation in the HFO-bearing sludge system was remarkable, with evidence of aromatic ring cleavage and no analytical evidence of the commonly observed aromatic amines. HFO-sludges present an efficient biogeochemically poised system for anaerobic decolourisation and concurrent biodegradation of the dyes through combinations of both reductive and oxidative attack by consortia of bacteria including Fe-reducers and the associated organic and inorganic reductants generated in the HFO system. Biodegradation seen in all systems tested suggests an indiscriminate biodegradation mechanism that might be widely applicable in dye-effluent treatment. The fact that these reactions occurred in a widely available common waste product in a simple packed bed reactor is highly advantageous as it would lead to their use in simple and sustainable passive treatment schemes for dye-bearing effluents. This may be particularly important to developing economies where the treatment of dye-bearing effluents has been limited.

Credit author statement

Pallavee Srivastava (First Author): Writing – original draft; Visualization; Formal analysis. **Safaa A Al-Obaidi** (First Author): Methodology; Validation; Formal analysis; Investigation. **Gordon Webster**: Methodology, Validation, and Formal analysis (for microbial community analysis); Writing – review & editing. **Andrew J Weightman**: Methodology, Validation, and Formal analysis (for microbial community analysis); Writing – review & editing. **Devin J Sapsford**: Conceptualization; Methodology; Writing – original draft; Visualization; Supervision; Funding acquisition; Project administration

Declaration of competing interest

The authors declare that they have no known competing financial interests or personal relationships that could have appeared to influence the work reported in this paper.

Acknowledgements

We would like to thank the following: Jeff Rowlands (Cardiff University, School of Engineering) for analytical support; The Iraqi Embassy and Ministry of Higher-Education and Scientific Research for funding for Al-Obaidi; Dŵr Cymru Welsh Water and The Coal Authority for the provision of waste sludges; Dr Ben Ward, Dr Rob Jenkins, and Tom Williams (Cardiff University, School of Chemistry) for LC-MS advice and provision of LC-MS analyses respectively; To the EPSRC UK National Mass Spectrometry Facility (Swansea University, UK). Aspects of the work were supported by the Natural Environmental Research Council [grant number: NE/L013908/1].

Appendix A. Supplementary data

Supplementary data to this article can be found online at https://doi.org/10.1016/j.jenvman.2022.115332.

References

16 S Illumina Amplicon Protocol : earthmicrobiome. n.d.Retrieved December 13, 2021. https://earthmicrobiome.org/protocols-and-standards/16s/. from.

Albuquerque, M.G.E., Lopes, A.T., Serralheiro, M.L., Novais, J.M., Pinheiro, H.M., 2005. Biological sulphate reduction and redox mediator effects on azo dye decolourisation in anaerobic-aerobic sequencing batch reactors. Enzym. Microb. Technol. 36 (5–6), 790–799. https://doi.org/10.1016/j.enzmictec.2005.01.005.

Altschul, S.F., Gish, W., Miller, W., Myers, E.W., Lipman, D.J., 1990. Basic local alignment search tool. J. Mol. Biol. 215 (3), 403–410. https://doi.org/10.1016/S0022-2836(05)80360-2.

Alzaydien, A.S., 2015. Adsorption behavior of methyl orange onto wheat bran: role of surface and pH. Orient. J. Chem. 31 (2), 643–651. https://doi.org/10.13005/ojc/310205.

Amaral, F.M., Kato, M.T., Florêncio, L., Gavazza, S., 2014. Color, organic matter and sulfate removal from textile effluents by anaerobic and aerobic processes. Bioresour. Technol. 163, 364–369. https://doi.org/10.1016/j.biortech.2014.04.026.

Ananthashankar, R., A G, 2013. Production, characterization and treatment of textile effluents: a critical review. J. Chem. Eng. Process Technol. 1–18. https://doi.org/10.4172/2157-7048.1000182, 0501.

Anjaneyulu, Y., Sreedhara Chary, N., Samuel Suman Raj, D., 2005. Decolourization of industrial effluents - available methods and emerging technologies - a review. Rev. Environ. Sci. Biotechnol. 4 (4), 245–273. https://doi.org/10.1007/s11157-005-1246-z.

Arora, P.K., 2015. Bacterial degradation of monocyclic aromatic amine. Front. Microbiol. 6 https://doi.org/10.3389/fmicb.2015.00820. Issue JUL.

Ayed, L., Khelifi, E., Jannet, H. Ben, Miladi, H., Cheref, A., Achour, S., Bakhrouf, A., 2010. Response surface methodology for decolorization of azo dye Methyl Orange by bacterial consortium: produced enzymes and metabolites characterization. Chem. Eng. J. 165 (1), 200–208. https://doi.org/10.1016/J.CEJ.2010.09.018.

Bafana, A., Chakrabarti, T., Muthal, P., Kanade, G., 2009. Detoxification of benzidine-based azo dye by E. gallinarum: time-course study. Ecotoxicol. Environ. Saf. 72 (3), 960–964. https://doi.org/10.1016/j.ecoenv.2007.11.013.

Bafana, A., Devi, S.S., Chakrabarti, T., 2011. Azo dyes: past, present and the future. Environ. Rev. 19 (NA), 350–371. https://doi.org/10.1139/a11-018.

Bailey, M.T., Moorhouse, A.M.L., Byrom, A.J., Kershaw, S., 2013. Applications for hydrous ferric oxide mine water treatment sludge - a review. In: Reliable Mine Water Technology: Proceedings of the International Mine Water Association Annual Conference, I, pp. 519–524, 2013& Ii, 63(January 2013).

Baken, S., Sjöstedt, C., Gustafsson, J.P., Seuntjens, P., Desmet, N., De Schutter, J., Smolders, E., 2013. Characterisation of hydrous ferric oxides derived from iron-rich groundwaters and their contribution to the suspended sediment of streams. Appl. Geochem. 39 (2013), 59–68. https://doi.org/10.1016/j.apgeochem.2013.09.013.

Balapure, K., Bhatt, N., Madamwar, D., 2015. Mineralization of reactive azo dyes present in simulated textile waste water using down flow microaerophilic fixed film bioreactor. Bioresour. Technol. 175, 1–7. https://doi.org/10.1016/j.biortech.2014.10.040.

Barnes, A., 2008. The rates and mechanisms of Fe (ll) oxidation in a passive vertical flow reactor for the treatment of ferruginous mine water. September.

Bearcock, J.M., Perkins, W.T., Dinelli, E., Wade, S.C., 2006. Fe(II)/Fe(III) 'green rust' developed within ochreous coal mine drainage sediment in South Wales, UK. Mineral. Mag. 70 (6), 731–741. https://doi.org/10.1180/0026461067060360.

Bhattacharya, A., Goyal, N., Gupta, A., 2017. Degradation of azo dye methyl red by alkaliphilic, halotolerant Nesterenkonia lacusekhoensis EMLA3: application in alkaline and salt-rich dyeing effluent treatment. Extremophiles 21, 479–490. https://doi.org/10.1007/s00792-017-0918-2.

Bheemaraddi, M.C., Patil, S., Shivannavar, C.T., Gaddad, S.M., 2014. Isolation and characterization of paracoccus sp. gsm2 capable of degrading textile azo dye reactive violet 5. https://doi.org/10.1155/2014/410704.

Breithaupt, T., Reemtsma, T., Jekel, M., Storm, T., Wiesmann, U., 2003. Combined biological treatment/ozonation of wastewaters for the mineralisation of non-

biodegradable naphthalene-1,5-disulphonic acid. Acta Biotechnol. 23 (4), 321–333. https://doi.org/10.1002/abio.200390041.
Bromley-Challenor, K.C.A., Knapp, J.S., Zhang, Z., Gray, N.C.C., Hetheridge, M.J., Evans, M.R., 2000. Decolorization of an azo dye by unacclimated activated sludge under anaerobic conditions. Water Res. 34 (18), 4410–4418. https://doi.org/10.1016/S0043-1354(00)00212-8.
Brown, D., Hamburger, B., 1987. The degradation of dyestuffs: Part III - investigations of their ultimate degradability. Chemosphere 16 (7), 1539–1553. https://doi.org/10.1016/0045-6535(87)90094-4.
Buchwald, C., Grabb, K., Hansel, C.M., Wankel, S.D., 2016. Constraining the role of iron in environmental nitrogen transformations: dual stable isotope systematics of abiotic NO2- reduction by Fe(II) and its production of N2O. Geochem. Cosmochim. Acta 186, 1–12. https://doi.org/10.1016/j.gca.2016.04.041.
Cai, P.J., Xiao, X., He, Y.R., Li, W.W., Chu, J., Wu, C., He, M.X., Zhang, Z., Sheng, G.P., Lam, M.H.W., Xu, F., Yu, H.Q., 2012. Anaerobic biodecolorization mechanism of methyl orange by Shewanella oneidensis MR-1. Appl. Microbiol. Biotechnol. 93 (4), 1769–1776. https://doi.org/10.1007/s00253-011-3508-8.
Caporaso, J.G., Kuczynski, J., Stombaugh, J., Bittinger, K., Bushman, F.D., Costello, E.K., Fierer, N., Peña, A.G., Goodrich, J.K., Gordon, J.I., Huttley, G.A., Kelley, S.T., Knights, D., Koenig, J.E., Ley, R.E., Lozupone, C.A., Mcdonald, D., Muegge, B.D., Pirrung, M., Knight, R., 2010. Correspondence QIIME allows analysis of high-throughput community sequencing data Intensity normalization improves color calling in SOLiD sequencing. Nat. Publish. Group 7 (5), 335–336. https://doi.org/10.1038/nmeth0510-335.
Caporaso, J.G., Lauber, C.L., Walters, W.A., Berg-Lyons, D., Huntley, J., Fierer, N., Owens, S.M., Betley, J., Fraser, L., Bauer, M., Gormley, N., Gilbert, J.A., Smith, G., Knight, R., 2012. Ultra-high-throughput microbial community analysis on the Illumina HiSeq and MiSeq platforms. ISME J. 6 (8), 1621–1624. https://doi.org/10.1038/ismej.2012.8.
Carmen, Z., Daniel, S., 2012. Textile organic dyes – characteristics, polluting effects and separation/elimination procedures from industrial effluents – a critical overview. In: Organic Pollutants Ten Years After the Stockholm Convention - Environmental and Analytical Update. https://doi.org/10.5772/32373.
Chan, Y.J., Chong, M.F., Law, C.L., Hassell, D.G., 2009. A review on anaerobic-aerobic treatment of industrial and municipal wastewater. Chem. Eng. J. 155 (1–2), 1–18. https://doi.org/10.1016/j.cej.2009.06.041.
Chang, J.S., Chen, B.Y., Lin, Y.S., 2004. Stimulation of bacterial decolorization of an azo dye by extracellular metabolites from Escherichia coli strain NO3. Bioresour. Technol. 91 (3), 243–248. https://doi.org/10.1016/S0960-8524(03)00196-2.
Chen, K.C., Wu, J.Y., Liou, D.J., Hwang, S.C.J., 2003. Decolorization of the textile dyes by newly isolated bacterial strains. J. Biotechnol. 101 (1), 57–68. https://doi.org/10.1016/S0168-1656(02)00303-6.
Chen, H., Wang, R.F., Cerniglia, C.E., 2004. Molecular cloning, overexpression, purification, and characterization of an aerobic FMN-dependent azoreductase from Enterococcus faecalis. Protein Expr. Purif. 34 (2), 302–310. https://doi.org/10.1016/j.pep.2003.12.016.
Chen, Y., Zhang, L., Feng, L., Chen, G., Wang, Y., Zhai, Z., Zhang, Q., 2019. Exploration of the key functional strains from an azo dye degradation microbial community by DGGE and high-throughput sequencing technology. Environ. Sci. Pollut. Control Ser. 26 (24), 24658–24671. https://doi.org/10.1007/s11356-019-05781-z.
Chung, K.T., Fulk, G.E., Egan, M., 1978. Reduction of azo dyes by intestinal anaerobes. Appl. Environ. Microbiol. 35 (3), 558–562. https://doi.org/10.1128/aem.35.3.558-562.1978.
Clomburg, J.M., Gonzalez, R., 2013. Anaerobic fermentation of glycerol: a platform for renewable fuels and chemicals. Trends Biotechnol. 31 (1), 20–28. https://doi.org/10.1016/j.tibtech.2012.10.006.
Comeau, A.M., Vincent, W.F., Bernier, L., Lovejoy, C., 2016. Novel chytrid lineages dominate fungal sequences in diverse marine and freshwater habitats. Sci. Rep. 6, 1–6. https://doi.org/10.1038/srep30120.
Coughlin, M.F., Kinkle, B.K., Bishop, P.L., 1999. Degradation of azo dyes containing aminonaphthol by Sphingomonas sp strain 1CX. J. Ind. Microbiol. Biotechnol. 23 (4–5), 341–346. https://doi.org/10.1038/sj.jim.2900746.
De León, K.B., Utturkar, S.M., Camilleri, L.B., Elias, D.A., Arkin, A.P., Fields, M.W., Brown, S.D., Wall, J.D., 2015. Complete genome sequence of Pelosinus fermentans JBW45, a member of a remarkably competitive group of Negativicutes in the Firmicutes phylum. Genome Announc. 3 (5) https://doi.org/10.1128/genomeA.01090-15.
Delforno, T.P., Okada, D.Y., Faria, C.V., Varesche, M.B.A., 2016. Evaluation of anionic surfactant removal in anaerobic reactor with Fe(III) supplementation. J. Environ. Manag. 183 (3), 687–693. https://doi.org/10.1016/j.jenvman.2016.09.026.
Dhaouefi, Z., Toledo-Cervantes, A., García, D., Bedoui, A., Ghedira, K., Chekir-Ghedira, L., Muñoz, R., 2018. Assessing textile wastewater treatment in an anoxic-aerobic photobioreactor and the potential of the treated water for irrigation. Algal Res. 29 (August 2017), 170–178. https://doi.org/10.1016/j.algal.2017.11.032.
Doğan, M., Alkan, M., Türkyilmaz, A., Özdemir, Y., 2004. Kinetics and mechanism of removal of methylene blue by adsorption onto perlite. J. Hazard Mater. 109 (1–3), 141–148. https://doi.org/10.1016/j.jhazmat.2004.03.003.
Du, L.N., Li, G., Zhao, Y.H., Xu, H.K., Wang, Y., Zhou, Y., Wang, L., 2015. Efficient metabolism of the azo dye methyl orange by Aeromonas sp. strain DH-6: characteristics and partial mechanism. Int. Biodeterior. Biodegrad. 105, 66–72. https://doi.org/10.1016/j.ibiod.2015.08.019.
Elsner, M., Schwarzenbach, R.P., Haderlein, S.B., 2004. Reactivity of Fe(II)-Bearing minerals toward reductive transformation of organic contaminants. Environ. Sci. Technol. 38 (3), 799–807. https://doi.org/10.1021/es0345569.
Fan, H.J., Lu, C.S., Lee, W.L.W., Chiou, M.R., Chen, C.C., 2011. Mechanistic pathways differences between P25-TiO2 and Pt-TiO2 mediated CV photodegradation. J. Hazard Mater. 185 (1), 227–235. https://doi.org/10.1016/j.jhazmat.2010.09.022.
Feng, W., Nansheng, D., Helin, H., 2000. Degradation mechanism of azo dye C. I. reactive red 2 by iron powder reduction and photooxidation in aqueous solutions. Chemosphere 41 (8), 1233–1238. https://doi.org/10.1016/S0045-6535(99)00538-X.
Firmino, P.I.M., da Silva, M.E.R., Cervantes, F.J., dos Santos, A.B., 2010. Colour removal of dyes from synthetic and real textile wastewaters in one- and two-stage anaerobic systems. Bioresour. Technol. 101 (20), 7773–7779. https://doi.org/10.1016/j.biortech.2010.05.050.
Forss, J., Pinhassi, J., Lindh, M., Welander, U., 2013. Microbial diversity in a continuous system based on rice husks for biodegradation of the azo dyes Reactive Red 2 and Reactive Black 5. Bioresour. Technol. 130, 681–688. https://doi.org/10.1016/J.BIORTECH.2012.12.097.
Fuller, S.J., McMillan, D.G.G., Renz, M.B., Schmidt, M., Burke, I.T., Stewart, D.I., 2014. Extracellular electron transport-mediated fe(iii) reduction by a community of alkaliphilic bacteria that use flavins as electron shuttles. Appl. Environ. Microbiol. 80 (1), 128–137. https://doi.org/10.1128/AEM.02282-13.
Ganesh, R., Boardman, G.D., Michelsen, D., 1994. Fate of azo dyes in sludges. Water Res. 28 (6), 1367–1376. https://doi.org/10.1016/0043-1354(94)90303-4.
García-Martínez, Y., Bengoa, C., Stüber, F., Fortuny, A., Font, J., Fabregat, A., 2015. Biodegradation of acid orange 7 in an anaerobic-aerobic sequential treatment system. Chem. Eng. Process: Process Intensif. 94, 99–104. https://doi.org/10.1016/j.cep.2014.12.011.
Garg, N., Garg, A., Mukherji, S., 2020. Eco-friendly decolorization and degradation of reactive yellow 145 textile dye by Pseudomonas aeruginosa and Thiosphaera pantotropha. J. Environ. Manag. 263, 110383. https://doi.org/10.1016/J.JENVMAN.2020.110383.
Georgiou, D., Metallinou, C., Aivasidis, A., Voudrias, E., Gimouhopoulos, K., 2004. Decolorization of azo-reactive dyes and cotton-textile wastewater using anaerobic digestion and acetate-consuming bacteria. Biochem. Eng. J. 19 (1), 75–79. https://doi.org/10.1016/j.bej.2003.11.003.
Govindaswami, M., Schmidt, T.M., White, D.C., Loper, J.C., 1993. Phylogenetic analysis of a bacterial aerobic degrader of azo dyes. J. Bacteriol. 175 (18), 6062–6066. https://doi.org/10.1128/jb.175.18.6062-6066.1993.
Guo, J., Zhou, J., Wang, D., Tian, C., Wang, P., Salah Uddin, M., Yu, H., 2007. Biocalalyst effects of immobilized anthraquinone on the anaerobic reduction of azo dyes by the salt-tolerant bacteria. Water Res. 41 (2), 426–432. https://doi.org/10.1016/j.watres.2006.10.022.
Guo, J., Kang, L., Wang, X., Yang, J., 2010. Decolorization and degradation of azo dyes by redox mediator system with bacteria (pp. 85–100. https://doi.org/10.1007/698_2009_46.
Han, R., Lv, J., Huang, Z., Zhang, S., Zhang, S., 2020. Pathway for the production of hydroxyl radicals during the microbially mediated redox transformation of iron (Oxyhydr)oxides. Environ. Sci. Technol. 54 (2), 902–910. https://doi.org/10.1021/acs.est.9b06220.
He, F., Hu, W., Li, Y., 2004. Biodegradation mechanisms and kinetics of azo dye 4BS by a microbial consortium. Chemosphere 57 (4), 293–301. https://doi.org/10.1016/j.chemosphere.2004.06.036.
Hisaindee, S., Meetani, M.A., Rauf, M.A., 2013. Application of LC-MS to the analysis of advanced oxidation process (AOP) degradation of dye products and reaction mechanisms. Trac. Trends Anal. Chem. 49, 31–44. https://doi.org/10.1016/j.trac.2013.03.011.
Hong, Y., Chen, X., Guo, J., Xu, Z., Xu, M., Sun, G., 2007. Effects of electron donors and acceptors on anaerobic reduction of azo dyes by Shewanella decolorationis S12. Appl. Microbiol. Biotechnol. 74 (1), 230–238. https://doi.org/10.1007/s00253-006-0657-2.
Igarashi, K., Kato, S., 2021. Reductive transformation of Fe(III) (oxyhydr)Oxides by mesophilic homoacetogens in the genus Sporomusa. Front. Microbiol. 12 https://doi.org/10.3389/fmicb.2021.600808.
Isaka, K., Sumino, T., Tsuneda, S., 2007. High nitrogen removal performance at moderately low temperature utilizing anaerobic ammonium oxidation reactions. J. Biosci. Bioeng. 103 (5), 486–490. https://doi.org/10.1263/jbb.103.486.
Işik, M., Sponza, D.T., 2005. Effects of alkalinity and co-substrate on the performance of an upflow anaerobic sludge blanket (UASB) reactor through decolorization of Congo Red azo dye. Bioresour. Technol. 96 (5), 633–643. https://doi.org/10.1016/j.biortech.2004.06.004.
Jamshidi, E., Manteghi, F., 2020. Methyl orange adsorption by Fe2O3@Co-Al-layered double hydroxide. Proceedings *41* (1), 64. https://doi.org/10.3390/ecsoc-23-06617.
Jin, D., Kong, X., Li, Y., Bai, Z., Zhuang, G., Zhuang, X., Deng, Y., 2015. Biodegradation of di-n-Butyl phthalate by achromobacter sp. isolated from rural domestic wastewater. OPEN ACCESS Int. J. Environ. Res. Public Health 12 (12). https://doi.org/10.3390/ijerph121013510.
Kadam, S.K., Chandanshive, V.V., Rane, N.R., Patil, S.M., Gholave, A.R., Khandare, R.V., Bhosale, A.R., Jeon, B.H., Govindwar, S.P., 2018. Phytobeds with Fimbristylis dichotoma and Ammannia baccifera for treatment of real textile effluent: an in situ treatment, anatomical studies and toxicity evaluation. Environ. Res. 160, 1–11. https://doi.org/10.1016/j.envres.2017.09.009. September.
Kalyani, D.C., Telke, A.A., Govindwar, S.P., Jadhav, J.P., 2009. Biodegradation and detoxification of reactive textile dye by isolated Pseudomonas sp. SUK1. Water Environ. Res. 81 (3), 298–307. https://doi.org/10.2175/106143008x357147.
Kant, R., 2012. Textile dyeing industry an environmental hazard. Nat. Sci. 22–26. https://doi.org/10.4236/ns.2012.41004, 0401.
Khalid, A., Kausar, F., Arshad, M., Mahmood, T., Ahmed, I., 2012. Accelerated decolorization of reactive azo dyes under saline conditions by bacteria isolated from

Arabian seawater sediment. Appl. Microbiol. Biotechnol. 96 (6), 1599–1606. https://doi.org/10.1007/s00253-012-3877-7.
Khan, R., Khan, Z., Nikhil, B., Jyoti, D., Datta, M., 2014. Azo dye decolorization under microaerophilic conditions by a bacterial mixture isolated from anthropogenic dye-contaminated soil. Ann. Finance 18 (2), 147–157. https://doi.org/10.1080/10889868.2014.889076.
Khandare, R.V., Govindwar, S.P., 2015. Phytoremediation of textile dyes and effluents: current scenario and future prospects. Biotechnol. Adv. 33 (8), 1697–1714. https://doi.org/10.1016/j.biotechadv.2015.09.003.
Kiliç, N.K., Nielsen, J.L., Yüce, M., Dönmez, G., 2007. Characterization of a simple bacterial consortium for effective treatment of wastewaters with reactive dyes and Cr(VI). Chemosphere 67 (4), 826–831. https://doi.org/10.1016/j.chemosphere.2006.08.041.
Kim, S.-Y., An, J.-Y., Kim, B.-W., 2008. The effects of reductant and carbon source on the microbial decolorization of azo dyes in an anaerobic sludge process. Dyes Pigments 76 (1), 256–263. https://doi.org/10.1016/j.dyepig.2006.08.042.
Kone, T., Hanna, K., Abdelmoula, M., Ruby, C., Carteret, C., 2009. Reductive transformation and mineralization of an azo dye by hydroxysulphate green rust preceding oxidation using H2O2 at neutral pH. Chemosphere 75 (2), 212–219. https://doi.org/10.1016/j.chemosphere.2008.12.002.
Kumar, A., 1998. Feminization of androecious papaya leading to fruit set by ethrel and chlorflurenol. Acta Hortic. 463, 251–259. https://doi.org/10.17660/actahortic.1998.463.30.
Le, C.P., Nguyen, H.T., Nguyen, T.D., Nguyen, Q.H.M., Pham, H.T., Dinh, H.T., 2021. Ammonium and organic carbon co-removal under feammox-coupled-with-heterotrophy condition as an efficient approach for nitrogen treatment. Scientific Reports, 11(1) 784. https://doi.org/10.1038/s41598-020-80057-y.
Li, S., Cao, Y., Bi, C., Zhang, Y., 2017. Promoting electron transfer to enhance anaerobic treatment of azo dye wastewater with adding Fe(OH)3. Bioresour. Technol. 245, 138–144. https://doi.org/10.1016/J.BIORTECH.2017.08.066.
Li, H., Tang, C., Wang, M., Mei, C., Liu, N., 2021. Decolorization of azo dyes in a heterogeneous persulfate system using FeS as the activator. Water Sci. Technol. 83 (7), 1703–1713. https://doi.org/10.2166/wst.2021.085.
Liu, G., Zhou, J., Wang, J., Wang, X., Jin, R., Lv, H., 2011. Decolorization of azo dyes by Shewanella oneidensis MR-1 in the presence of humic acids. Appl. Microbiol. Biotechnol. 91 (2), 417–424. https://doi.org/10.1007/s00253-011-3273-8.
Liu, Y., Zhang, Y., Zhao, Z., Li, Y., Quan, X., Chen, S., 2012. Enhanced azo dye wastewater treatment in a two-stage anaerobic system with Fe0 dosing. Bioresour. Technol. 121, 148–153. https://doi.org/10.1016/j.biortech.2012.06.115.
Liu, W., Liu, L., Liu, C., Hao, Y., Yang, H., Yuan, B., Jiang, J., 2016. Methylene blue enhances the anaerobic decolorization and detoxication of azo dye by Shewanella onediensis MR-1. Biochem. Eng. J. 110, 115–124. https://doi.org/10.1016/J.BEJ.2016.02.012.
Liu, J., Xiong, J., Tian, C., Gao, B., Wang, L., Jia, X., 2018. The degradation of methyl orange and membrane fouling behavior in anaerobic baffled membrane bioreactor. Chem. Eng. J. 338, 719–725. https://doi.org/10.1016/J.CEJ.2018.01.052.
Lovley, D.R., Giovannoni, S.J., White, D.C., Champine, J.E., Phillips, E.J.P., Gorby, Y.A., Goodwin, S., 1993. Geobacter metallireducens gen. nov. sp. nov., a microorganism capable of coupling the complete oxidation of organic compounds to the reduction of iron and other metals. Arch. Microbiol. 159 (4), 336–344. https://doi.org/10.1007/BF00290916.
Luu, Y.S., Ramsay, J.A., 2003. Review: microbial mechanisms of accessing insoluble Fe (III) as an energy source. World J. Microbiol. Biotechnol. 19 (2), 215–225. https://doi.org/10.1023/A:1023225521311.
Mia, R., Selim, M., Shamim, A.M., Chowdhury, M., Sultana, S., Armin, M., Hossain, M., Akter, R., Dey, S., Naznin, H., 2019. Review on various types of pollution problem in textile dyeing & printing industries of Bangladesh and recommandation for mitigation. J. Textile Eng. Fashion Technol. 5 (4), 220–226. https://doi.org/10.15406/jteft.2019.05.00205.
Moe, W.M., Stebbing, R.E., Rao, J.U., Bowman, K.S., Fernanda Nobre, M., da Costa, M.S., Rainey, F.A., 2012. Pelosinus defluvii sp. nov., isolated from chlorinated solvent-contaminated groundwater, emended description of the genus Pelosinus and transfer of Sporotalea propionica to Pelosinus propionicus comb. nov. Int. J. Syst. Evol. Microbiol. 62 (6), 1369–1376. https://doi.org/10.1099/ijs.0.033753-0.
Murali, V., Ong, S.A., Ho, L.N., Wong, Y.S., 2013a. Decolorization of methyl orange using upflow anaerobic sludge blanket (UASB) reactor-An investigation of co-substrate and dye degradation kinetics. Desalination Water Treat. 51 (40–42), 7621–7630. https://doi.org/10.1080/19443994.2013.782255.
Murali, V., Ong, S.A., Ho, L.N., Wong, Y.S., 2013b. Evaluation of integrated anaerobic-aerobic biofilm reactor for degradation of azo dye methyl orange. Bioresour. Technol. 143, 104–111. https://doi.org/10.1016/j.biortech.2013.05.122.
Namasivayam, C., Arasi, D.J.S.E., 1997. Removal of Congo red from wastewater by adsorption onto waste red mud. Chemosphere 34 (2), 401–417. https://doi.org/10.1016/S0045-6535(96)00385-2.
Nigam, P., Banat, I.M., Singh, D., Marchant, R., 1996. Microbial process for the decolorization of textile effluent containing azo, diazo and reactive dyes. Process Biochem. 31 (5), 435–442. https://doi.org/10.1016/0032-9592(95)00085-2.
Oon, Y.L., Ong, S.A., Ho, L.N., Wong, Y.S., Dahalan, F.A., Oon, Y.S., Lehl, H.K., Thung, W.E., Nordin, N., 2018. Up-flow constructed wetland-microbial fuel cell for azo dye, saline, nitrate remediation and bioelectricity generation: from waste to energy approach. Bioresour. Technol. 266 (April), 97–108. https://doi.org/10.1016/j.biortech.2018.06.035.
Ottley, C.J., Davison, W., Edmunds, W.M., 1997. Chemical catalysis of nitrate reduction by iron (II). Geochem. Cosmochim. Acta 61 (9), 1819–1828. https://doi.org/10.1016/S0016-7037(97)00058-6.
Oturkar, C.C., Nemade, H.N., Mulik, P.M., Patole, M.S., Hawaldar, R.R., Gawai, K.R., 2011. Mechanistic investigation of decolorization and degradation of Reactive Red 120 by Bacillus lentus BI377. Bioresour. Technol. 102 (2), 758–764. https://doi.org/10.1016/j.biortech.2010.08.094.
O'Neill, C., Hawkes, F.R., Hawkes, D.L., Esteves, S., Wilcox, S.J., 2000. Anaerobic-aerobic biotreatment of simulated textile effluent containing varied ratios of starch and azo dye. Water Res. 34 (8), 2355–2361. https://doi.org/10.1016/S0043-1354(99)00395-4.
Pandey, A., Singh, P., Iyengar, L., 2007. Bacterial decolorization and degradation of azo dyes. Int. Biodeterior. Biodegrad. 59 (2), 73–84. https://doi.org/10.1016/J.IBIOD.2006.08.006.
Parshetti, G.K., Telke, A.A., Kalyani, D.C., Govindwar, S.P., 2010. Decolorization and detoxification of sulfonated azo dye methyl orange by Kocuria rosea MTCC 1532. J. Hazard Mater. 176 (1–3), 503–509. https://doi.org/10.1016/j.jhazmat.2009.11.058.
Pattrick, R.A.D., Coker, V.S., Pearce, C.I., Telling, N.D., van der Laan, G., Lloyd, J.R., 2013. Extracellular bacterial production of doped magnetite nanoparticles. In *Nanoscience: Volume 1: Nanostructures through Chemistry* Vol. 1, 102–115. https://doi.org/10.1039/9781849734844-00102. The Royal Society of Chemistry.
Pinheiro, H.M., Touraud, E., Thomas, O., 2004. Aromatic amines from azo dye reduction: status review with emphasis on direct UV spectrophotometric detection in textile industry wastewaters. Dyes Pigments 61 (2), 121–139. https://doi.org/10.1016/j.dyepig.2003.10.009.
Plumb, J.J., Bell, J., Stuckey, D.C., 2001. Microbial populations associated with treatment of an industrial dye effluent in an anaerobic baffled reactor. Appl. Environ. Microbiol. 67 (7), 3226–3235. https://doi.org/10.1128/AEM.67.7.3226-3235.2001.
Punj, S., John, G.H., 2009. Purification and identification of an FMN-dependent NAD(P)H azoreductase from Enterococcus faecalis. Curr. Issues Mol. Biol. 11, 59–66. https://doi.org/10.21775/cimb.011.059.
Rasool, K., Shahzad, A., Lee, D.S., 2016. Exploring the potential of anaerobic sulfate reduction process in treating sulfonated diazo dye: microbial community analysis using bar-coded pyrosequencing. J. Hazard Mater. 318, 641–649. https://doi.org/10.1016/j.jhazmat.2016.07.052.
Reeves, R.L., Kaiser, R.S., Maggio, M.S., Sylvestre, E.A., Lawton, W.H., 1973. Analysis of the visual spectrum of methyl orange in solvents and in hydrophobic binding sites. Can. J. Chem. 51 (4), 628–635. https://doi.org/10.1139/v73-095.
Redmann, R.E., 1978. Canadian journal. Can. J. Soil Sci. 58 (May), 119–124.
Roberts, M., 2018. In-Situ microbial Dissolution of iron mineral-bearing Wastes for metal recovery. June.
Rosenberg, E., DeLong, E.F., Lory, S., Stackebrandt, E., Thompson, F., 2013. The prokaryotes - prokaryotic biology and symbiotic | eugene Rosenberg |. In the prokaryotes - prokaryotic biology and symbiotic. http://www.springer.com/us/book/9783642301933.
Rumky, J., 2013. Environmental treatment of dyes: methyl orange decolorization using hog plum peel and mix-bacterial strains. IOSR J. Environ. Sci. Toxicol. Food Technol. 5 (3), 19–22. https://doi.org/10.9790/2402-0531922.
Saratale, R.G., Saratale, G.D., Chang, J.S., Govindwar, S.P., 2011. Bacterial decolorization and degradation of azo dyes: a review. J. Taiwan Inst. Chem. Eng. 42 (1), 138–157. https://doi.org/10.1016/j.jtice.2010.06.006.
Schuppert, B., Schink, B., 1990. Fermentation of methoxyacetate to glycolate and acetate by newly isolated strains of Acetobacterium sp. Arch. Microbiol. 153 (2), 200–204. https://doi.org/10.1007/BF00247821.
Schwertmann, U., Cornell, R.M., Rao, C.N.R., Raveau, B., Jolivet, J.-P., Henry, M., Livage, J., 2003. Also of interest iron oxides in the laboratory transition metal oxides metal oxide chemistry and synthesis. Synthesis. http://dnb.ddb.de.
Silke, B., Matthias, C., Martina, L., Andreas, S., Hans-Joachim, K., 1998. Isolation of a bacterial strain with the ability to utilize the sulfonated azo compound 4-carboxy-4′-sulfoazobenzene as the sole source of carbon and energy. Appl. Environ. Microbiol. 64 (6), 2315–2317. https://doi.org/10.1128/AEM.64.6.2315-2317.1998.
Singh, B., Gräfe, M., Kaur, N., Liese, A., 2010. Applications of synchrotron-based X-ray diffraction and X-ray absorption spectroscopy to the understanding of poorly crystalline and metal-substituted Iron oxides. Dev. Soil Sci. 34, 199–254. https://doi.org/10.1016/s0166-2481(10)34008-6.
Singh, R.L., Singh, P.K., Singh, R.P., 2015. Enzymatic decolorization and degradation of azo dyes – a review. Int. Biodeterior. Biodegrad. 104, 21–31. https://doi.org/10.1016/J.IBIOD.2015.04.027.
Sorokin, D.Y., Tourova, T.P., Mußmann, M., Muyzer, G., 2008. Dethiobacter alkaliphilus gen. nov. sp. nov., and Desulfurivibrio alkaliphilus gen. nov. sp. nov.: two novel representatives of reductive sulfur cycle from soda lakes. Extremophiles 12 (3), 431–439. https://doi.org/10.1007/s00792-008-0148-8.
Stein, S.E., Linstrom, P., Mirokhin, Y., Tchekhovskoi, D., Yang, X., Gary, W., Sparkman, M.O.D., 2011. NIST 14 MS database and MS search program v.2.2 NIST standard reference database 1A NIST/EPA/NIH mass spectral library (NIST 14) and NIST mass spectral search program (version 2.2) for use with microsoft ® windows user's guide the NIST mass spectrometry D. Nist, June 2008, 1–49. https://www.nist.gov/sites/default/files/documents/srd/NIST1aVer22Man.pdf.
Stolz, A., 2001. Basic and applied aspects in the microbial degradation of azo dyes. Appl. Microbiol. Biotechnol. 56 (1–2), 69–80. https://doi.org/10.1007/s002530100686.
Tai, Y.L., Dempsey, B.A., 2009. Nitrite reduction with hydrous ferric oxide and Fe(II): stoichiometry, rate, and mechanism. Water Res. 43 (2), 546–552. https://doi.org/10.1016/j.watres.2008.10.055.
Telke, A.A., Kalyani, D.C., Dawkar, V.V., Govindwar, S.P., 2009. Influence of organic and inorganic compounds on oxidoreductive decolorization of sulfonated azo dye C.I. Reactive Orange 16. J. Hazard Mater. 172 (1), 298–309. https://doi.org/10.1016/j.jhazmat.2009.07.008.

Teramoto, E.H., Chang, H.K., 2019. Geochemical conceptual model of BTEX biodegradation in an iron-rich aquifer. Appl. Geochem. 100 (March 2018), 293–304. https://doi.org/10.1016/j.apgeochem.2018.11.019.

Texier, A.-C., Zepeda, A., Gmez, J., Cuervo-Lpez, F., 2012. Simultaneous elimination of carbon and nitrogen compounds of petrochemical effluents by nitrification and denitrification. Petrochemicals. https://doi.org/10.5772/37957.

Thao, T.P., Kao, H.C., Juang, R.S., Lan, J.C.W., 2013. Kinetic characteristics of biodegradation of methyl orange by Pseudomonas putida mt2 in suspended and immobilized cell systems. J. Taiwan Inst. Chem. Eng. 44 (5), 780–785. https://doi.org/10.1016/j.jtice.2013.01.015.

Tian, T., Yu, H.Q., 2020. Iron-assisted biological wastewater treatment: synergistic effect between iron and microbes. Biotechnol. Adv. 44 https://doi.org/10.1016/j.biotechadv.2020.107610.

Tobler, N.B., Hofstetter, T.B., Straub, K.L., Fontana, D., Schwarzenbach, R.P., 2007. Iron-mediated microbial oxidation and abiotic reduction of organic contaminants under anoxic conditions. Environ. Sci. Technol. 41 (22), 7765–7772. https://doi.org/10.1021/es071128k.

Vadivelan, V., Vasanth Kumar, K., 2005. Equilibrium, kinetics, mechanism, and process design for the sorption of methylene blue onto rice husk. J. Colloid Interface Sci. 286 (1), 90–100. https://doi.org/10.1016/j.jcis.2005.01.007.

van Beek, C.G.E.M., Hofman-Caris, C.H.M., Zweere, G.J., 2020. Drinking water treatment and chemical well clogging by iron(II) oxidation and hydrous ferric oxide (HFO) precipitation. J. Water Supply Res. Technol. - Aqua 69 (5), 427–437. https://doi.org/10.2166/aqua.2020.140.

Van Der Zee, F.P., Villaverde, S., 2005. Combined anaerobic-aerobic treatment of azo dyes - a short review of bioreactor studies. Water Res. 39 (8), 1425–1440. https://doi.org/10.1016/j.watres.2005.03.007.

Venosa, A.D., Zhu, X., 2003. Biodegradation of crude oil contaminating marine shorelines and freshwater wetlands. Spill Sci. Technol. Bull. 8 (2), 163–178. https://doi.org/10.1016/S1353-2561(03)00019-7.

Vymazal, J., 2007. Removal of nutrients in various types of constructed wetlands. Sci. Total Environ. 380 (1–3), 48–65. https://doi.org/10.1016/j.scitotenv.2006.09.014.

Vymazal, J., 2013. The use of hybrid constructed wetlands for wastewater treatment with special attention to nitrogen removal: a review of a recent development. Water Res. 47 (14), 4795–4811. https://doi.org/10.1016/j.watres.2013.05.029.

Wang, Z.W., Liang, J.S., Liang, Y., 2013. Decolorization of Reactive Black 5 by a newly isolated bacterium Bacillus sp. YZU1. Int. Biodeterior. Biodegrad. 76, 41–48. https://doi.org/10.1016/j.ibiod.2012.06.023.

Wang, Z., Yin, Q., Gu, M., He, K., Wu, G., 2018. Enhanced azo dye Reactive Red 2 degradation in anaerobic reactors by dosing conductive material of ferroferric oxide. J. Hazard Mater. 357, 226–234. https://doi.org/10.1016/J.JHAZMAT.2018.06.005.

Webster, G., Newberry, C.J., Fry, J.C., Weightman, A.J., 2003. Assessment of bacterial community structure in the deep sub-seafloor biosphere by 16S rDNA-based techniques: a cautionary tale. J. Microbiol. Methods 55 (1), 155–164. https://doi.org/10.1016/S0167-7012(03)00140-4.

Wei, Y., Dai, J., Mackey, H.R., Chen, G.H., 2017. The feasibility study of autotrophic denitrification with iron sludge produced for sulfide control. Water Res. 122, 226–233. https://doi.org/10.1016/j.watres.2017.05.073.

Wijetunga, S., Li, X.F., Jian, C., 2010. Effect of organic load on decolourization of textile wastewater containing acid dyes in upflow anaerobic sludge blanket reactor. J. Hazard Mater. 177 (1–3), 792–798. https://doi.org/10.1016/j.jhazmat.2009.12.103.

Willmott, N., 1998. To colour removal from. Jsdc 114 (2), 38–41.

Xiao, H., Peng, H., Yang, P., 2011. Performance of a new-type integrated biofilm reactor in treating high concentration organic wastewater. Procedia Environ. Sci. 11 (PART B), 674–679. https://doi.org/10.1016/j.proenv.2011.12.105.

Yadav, A.K., Jena, S., Acharya, B.C., Mishra, B.K., 2012. Removal of azo dye in innovative constructed wetlands: influence of iron scrap and sulfate reducing bacterial enrichment. Ecol. Eng. 49, 53–58. https://doi.org/10.1016/j.ecoleng.2012.08.032.

Yang, Q., Zhang, W., Zhang, H., Li, Y., Li, C., 2011. Wastewater treatment by alkali bacteria and dynamics of microbial communities in two bioreactors. Bioresour. Technol. 102 (4), 3790–3798. https://doi.org/10.1016/J.BIORTECH.2010.12.030.

Yang, W.H., Weber, K.A., Silver, W.L., 2012. Nitrogen loss from soil through anaerobic ammonium oxidation coupled to iron reduction. Nat. Geosci. 5 (8), 538–541. https://doi.org/10.1038/ngeo1530.

Yaseen, D.A., Scholz, M., 2018. Treatment of synthetic textile wastewater containing dye mixtures with microcosms. Environ. Sci. Pollut. Control Ser. 25 (2), 1980–1997. https://doi.org/10.1007/s11356-017-0633-7.

Yemashova, N., Kalyuzhnyi, S., 2006. Microbial conversion of selected azo dyes and their breakdown products. Water Sci. Technol. 53 (11), 163–171. https://doi.org/10.2166/wst.2006.349.

Yemashova, N.A., Kotova, I.B., Netrusov, A.I., Kalyuzhnyi, S.V., 2009. Special traits of decomposition of azo dyes by anaerobic microbial communities. Appl. Biochem. Microbiol. 45 (2), 176–181. https://doi.org/10.1134/S0003683809020100.

Yoo, E.S., 2002. Kinetics of chemical decolorization of the azo dye C.I. Reactive Orange 96 by sulfide. Chemosphere 47 (9), 925–931. https://doi.org/10.1016/S0045-6535(02)00068-1.

Yu, L., Li, W.W., Lam, M.H.W., Yu, H.Q., 2011. Adsorption and decolorization kinetics of methyl orange by anaerobic sludge. Appl. Microbiol. Biotechnol. 90 (3), 1119–1127. https://doi.org/10.1007/s00253-011-3109-6.

Yu, L., Zhang, X.Y., Wang, S., Tang, Q.W., Xie, T., Lei, N.Y., Chen, Y.L., Qiao, W.C., Li, W. W., Lam, M.H.W., 2015. Microbial community structure associated with treatment of azo dye in a start-up anaerobic sequenced batch reactor. J. Taiwan Inst. Chem. Eng. 54, 118–124. https://doi.org/10.1016/j.jtice.2015.03.012.

Yu, L., Wang, S., Tang, Q. wen, Cao, M. yue, Li, J., Yuan, K., Wang, P., Li, W. wei, 2016. Enhanced reduction of Fe(III) oxides and methyl orange by Klebsiella oxytoca in presence of anthraquinone-2-disulfonate. Appl. Microbiol. Biotechnol. 100 (10), 4617–4625. https://doi.org/10.1007/s00253-016-7281-6.

Zhang, Y., Jing, Y., Zhang, J., Sun, L., Quan, X., 2011. Performance of a ZVI-UASB reactor for azo dye wastewater treatment. J. Chem. Technol. Biotechnol. 86 (2), 199–204. https://doi.org/10.1002/jctb.2485.

Zhang, Y., Liu, Y., Jing, Y., Zhao, Z., Quan, X., 2012. Steady performance of a zero valent iron packed anaerobic reactor for azo dye wastewater treatment under variable influent quality. J. Environ. Sci. 24 (4), 720–727. https://doi.org/10.1016/S1001-0742(11)60803-6.

Zhu, Y., Cao, X., Cheng, Y., Zhu, T., 2018. Performances and structures of functional microbial communities in the mono azo dye decolorization and mineralization stages. Chemosphere 210, 1051–1060. https://doi.org/10.1016/j.chemosphere.2018.07.083.